IS-T-388

INFRARED SPECTRA OF SUBSTITUTIONAL H^- AND D^- IMPURITIES (U-CENTERS) IN CsBr AND CsI

Ph. D. Thesis Submitted to Iowa State University, August 1970

Clifford Gerald Olson

Ames Laboratory, USAEC

Iowa State University

Ames, Iowa 50010

PREPARED FOR U. S. ATOMIC ENERGY COMMISSION UNDER CONTRACT NO. W-7405-eng-82

Date Transmitted: October 1970

DISCLAIMER

IS-T-388

Printed in the United States of America
Available from
Clearinghouse for Federal Scientific and Technical Information
National Bureau of Standards, U.S. Department of Commerce
Springfield, Virginia 22151
Price: Printed Copy $3.00; Microfiche $0.65

INFRARED SPECTRA OF SUBSTITUTIONAL H^- AND D^- IMPURITIES (U-CENTERS) IN CsBr AND CsI

by

Clifford Gerald Olson

A Dissertation Submitted to the
Graduate Faculty in Partial Fulfillment of
The Requirements for the Degree of
DOCTOR OF PHILOSOPHY

Major Subject: Solid State Physics

Approved:

David W. Lynch
In Charge of Major Work

Head of Major Department

Dean of Graduate College

Iowa State University
Ames, Iowa

August 1970

INFRARED SPECTRA OF SUBSTITUTIONAL H^- AND D^- IMPURITIES (U-CENTERS) IN CsBr AND CsI

Clifford Gerald Olson

ABSTRACT

Hydrogen and deuterium U-centers were produced in CsBr and CsI. The low temperature sidebands were measured as well as the temperature dependence of the local mode frequency and the absorption half-width. The measured frequencies at the low temperature limit are: CsBr:H^-, 364.08 cm^{-1}; CsBr:D^-, 257.40 cm^{-1}; CsI:H^-, 283.5 cm^{-1}; CsI:D^-, 202. cm^{-1}. The CsBr and CsI U-centers have different temperature dependent properties.

The half-widths of both CsBr:H^- and CsBr:D^- have a T^2 temperature dependence. At high temperatures the width is due to modulation broadening involving the fourth order anharmonic term. The modulation term goes to zero at low temperatures and the residual width is determined by the decay of the CsBr:H^- local mode into four lattice modes and CsBr:D^- local mode into three. At low temperatures the energy of the absorption maximum varies linearly with T. The source

of this shift was not established although at higher temperatures thermal expansion apparently is the source of the deviation from a T dependence. The sidebands are very weak, but with an appropriate weighting factor they are in good agreement with a calculated one-phonon density of states.

With increasing temperature, the CsI U-center main peak absorption develops a high energy shoulder which grows rapidly in strength at the expense of what would normally be the local mode absorption. This asymmetry distorts the temperature dependence of the half-width and peak energy. No satisfactory explanation has been found for this adsorption.

TABLE OF CONTENTS

INTRODUCTION

A U-center is a very light ion, either hydrogen or deuterium, at a normal halogen lattice site of an alkali halide. The electronic properties of this defect have been studied for many years and are in general well known (1). The primary optical feature is an absorption band (U-band) in the ultraviolet at an energy slightly lower than that of the fundamental absorption edge of the crystal. Physically, this represents an electron bound less tightly to the hydrogen defect than other electrons are bound to the halogen atoms in the lattice.

In 1960 an infrared absorption corresponding to this same center was reported (2). Since the mass of the defect is so much less than the normal ionic mass, it will tend to vibrate at a frequency much higher than that of the normal lattice vibrations if the forces coupling it to the lattice are relatively unchanged. The mode represents the motion of a charged impurity at a site of cubic symmetry. The mode is optically active therefore, since it is associated with a non-zero dipole moment which can couple to the electromagnetic radiation. The vibration may be characterized as a localized mode. Since the frequency is much greater than any that can propagate through the lattice, the mode is restricted to the immediate vicinity of the defect.

CsBr and CsI both crystallize in the CsCl structure. That

is, there are cesium atoms at the eight corners of a cube with a halogen at the cube center. The unit cell is simple cubic with two atoms per unit cell, Cs at (0,0,0) and the halogen at $(\frac{1}{2}a,\frac{1}{2}a,\frac{1}{2}a)$ where a is the lattice constant. This means that the crystal has full cubic symmetry O_h and, in addition, the perfect crystal has translational invariance. This invariance gives rise to a conservation rule for the wave vector $\bar{k}$. The physical effect of this is to restrict first-order optical processes to k = 0 lattice phonons. (Typical infrared values for k are 10^3 cm^{-1} while for the lattice $k_{max} \approx 10^8 cm^{-1}$). A substitutional defect such as a U-center removes translational invariance and along with it, the wave vector selection rule. Because of this the mass defect will not only have a local mode absorption but will also produce absorption involving those lattice phonons that are permitted by symmetry. This extra absorption (sidebands) will be due to the creation of a local mode and the creation or absorption of a lattice mode.

In the perfect lattice the phonon is described by an irreducible representation of the space group of the lattice. To determine the selection rules it is necessary to reduce the symmetry of the space group to that of the point group of the defect site. This has been done by Loudon (3) for many crystal structures including NaCl, but not CsCl. The face centered cubic (fcc) symmetry does however have some points in common with the simple cubic. Thus groups associated with

Γ, Δ, Σ and Λ (Figure 1) are the same for both cases. In addition S and Z have the same space group as Δ (4) and X and M have the same space group as the point X in the fcc structure. Point R has the full cubic symmetry and is equivalent to Γ. Loudon's reduction table for fcc may therefore be used for most points of the simple cubic lattice.

The U-center local mode and the electric-dipole operator both have Γ_{15}^- symmetry. Therefore the U-center can only couple to a lattice mode whose representation contains one of the site groups

$$\Gamma_{15}^- \times \Gamma_{15}^- = \Gamma_1^+ + \Gamma_{12}^+ + \Gamma_{15}^+ + \Gamma_{25}^+ \ . \qquad (1\text{-}1)$$

(In other notation this is

$$T_1' \times T_1' = A_1 + E + T_1 + T_2 \ .) \qquad (1\text{-}2)$$

Warren (5) predicted a typical phonon structure for the CsCl lattice from symmetry considerations. The only discrepancy with curves calculated later by Karo and Hardy (6) (see Figures 2 and 3) involves the composition of degenerate modes at X. Later Cowley and Okazaki (7) measured the dispersion curves of TlBr, another CsCl structure material. The nature of the states at X agrees with Karo and Hardy. Cowley's symmetry assignments are used for X. Loudon's table shows that all possible representations of the space groups Σ, Δ, and Λ (and therefore S and Z) contain at least one of the site groups given in Equation (1-1) and all phonons at these

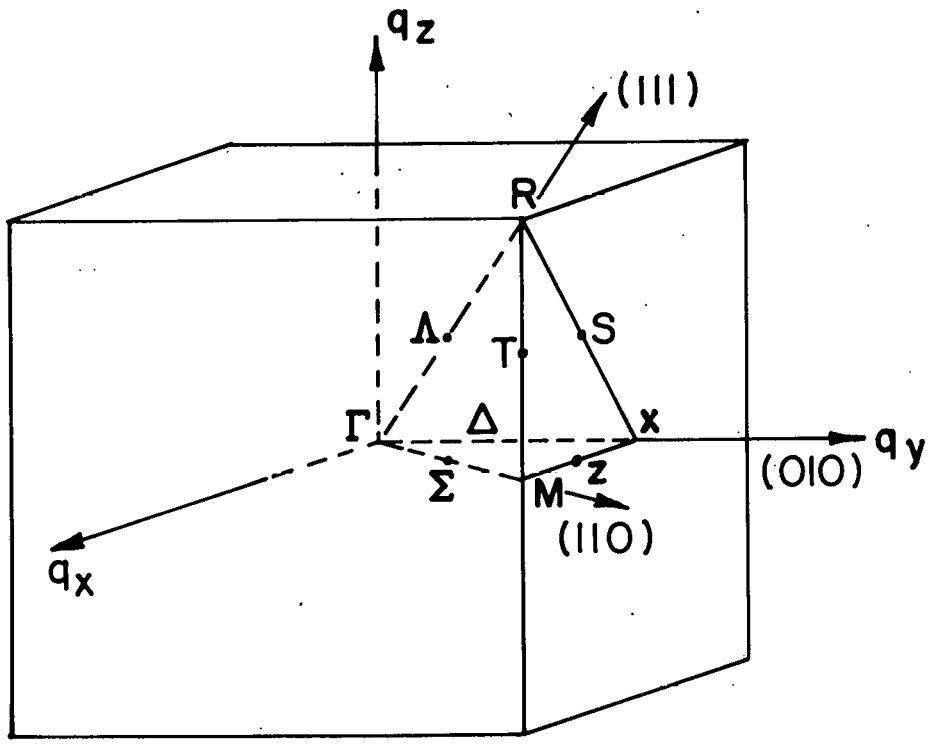

Figure 1. First Brillouin zone for simple cubic lattice showing symmetry axes and points

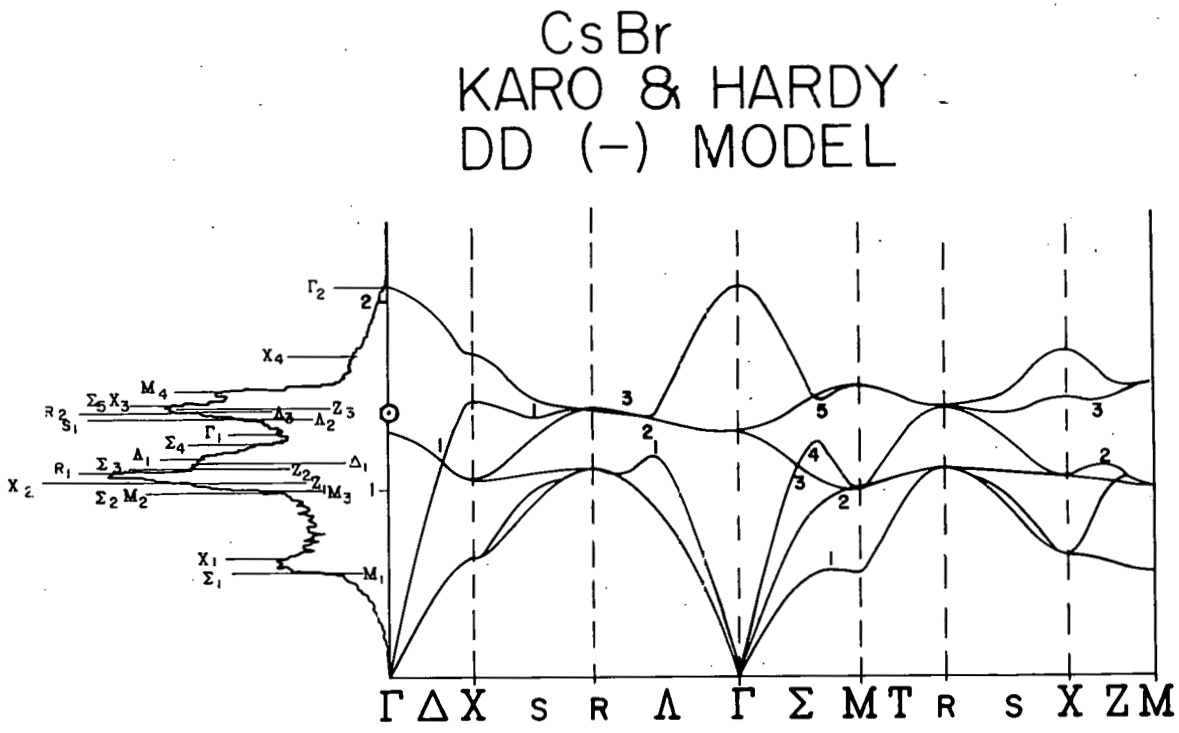

Figure 2. CsBr phonon frequency spectrum and dispersion curves calculated by Karo and Hardy

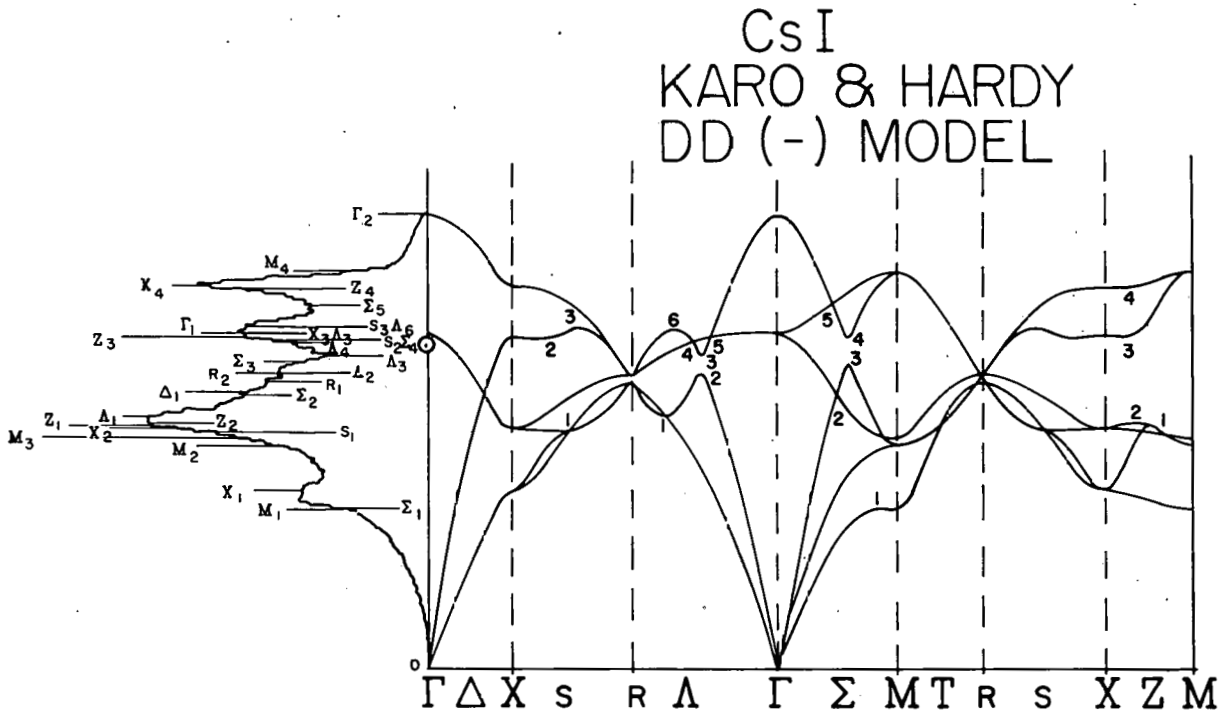

Figure 3. CsI phonon frequency spectrum and dispersion curves calculated by Karo and Hardy

symmetry points or lines will appear in the sideband spectra. The lower (acoustic) branch at R contributes, but not the upper. All points at M are forbidden. At site X coupling to the optic phonons is permitted but not to the acoustic.

Sidebands provide some of the most important information to be obtained from U-centers. Within the limitations of symmetry, sidebands provide a direct measure of the one-phonon density of states. This is especially important in Cs halides. Neutron diffraction studies are extremely difficult as the Cs ions are strongly absorbing. Specific heat measurements are useful but do not give the details available from sidebands. Only one calculation of Cs halide phonon dispersion curves is available. Karo and Hardy (6) have used three different models to calculate the effective dipole moments which enter into the long-range interaction. The rigid ion model assumes the ionic charges are rigid spheres which remain centered about the nuclei. The polarization dipole model assigns finite electronic polarizabilities to the ions. The deformation dipole model allows the ions to distort. In one approximation (DD(-)) only the negative ions deform. In another only positive ions deform (DD(+)). The authors felt their deformation dipole model gave the most satisfactory agreement with the specific heat data available. Data that will be given for CsBr sidebands argue strongly in favor of the DD(-) approximation. The calculated dispersion curves and one-phonon density of states are given in Figures 2 and 3.

A great deal of work has been done on local modes in the last ten years. Almost all of the experimental work has been done on NaCl structure lattices. Calculated dispersion curves are more abundant for these materials and many of the crystals have also been studied by inelastic neutron scattering. Also, the local mode absorptions occur at shorter wavelengths than in the CsCl salts and this is a definite experimental advantage. The only previous experimental measurements on Cs halide U-centers have been by Bauer (8), Mitra and Brada (9) and Dotsch and Mitra (10). An extensive bibliography and review of work on NaCl structure salts is contained in the proceedings of the First International Conference on Localized Excitations in Solids (1967) (11).

Theoretical literature on localized modes is equally vast. The simple mass defect model does not predict even the proper frequency for the local mode. It is necessary to introduce some effect equivalent to a change in the force constant between the defect and the host lattice. Harmonic approximations suffice to calculate the local mode energy. Beyond that, it is necessary to consider the anharmonic portion of the coupling in order to account for sidebands, broadening of the local mode and a shift of the mode energy with temperature. Many models, some of which will be discussed later, have been developed to account for these features. An extensive bibliography of theoretical work is contained in a review by Klein (12) of one of the force constant change models.

THEORY

The Hamiltonian of an otherwise perfect lattice containing a U-center may be written

$$H = H^{har} + H^{anhar} . \qquad (2\text{-}1)$$

The Hamiltonian may be expressed in terms of the position coordinates of the ions of the crystal. The position $\bar{r}$ of a given nucleus in a given cell may be written

$$\bar{r} = \bar{R} + \bar{u} \qquad (2\text{-}2)$$

where $\bar{R}$ is the equilibrium position and $\bar{u}$ is the displacement. Subscripts indicating the particular nucleus and cell are omitted. The harmonic Hamiltonian is

$$H^{har} = \tfrac{1}{2}\sum_i \Sigma m(\dot{u}_i)^2 + \tfrac{1}{2}\sum_{ij} \Sigma A^{(2)} u_i u_j \qquad (2\text{-}3)$$

where i and j are rectangular coordinates and the sum is also over all nuclei. $A^{(2)}$ is the second derivative of the potential energy evaluated at equilibrium. The anharmonic portion of the Hamiltonian is a sum of terms $(V^{(3)} + V^{(4)} + V^{(5)} + \ldots)$ of the form

$$V^{(3)} = \frac{1}{3!} \Sigma \Sigma A^{(3)} u_1 u_2 u_3 . \qquad (2\text{-}4)$$

$A^{(3)}$ is the third derivative and the sums are over rectangular coordinates and then all nuclei.

The displacement vectors u may be expanded in terms of the eigenvectors of the harmonic portion of the Hamiltonian (v_l) and the normal coordinates $q^l(t)$

$$\sqrt{m}\, u = \sum_l v_l q^l(t). \qquad (2\text{-}5)$$

Here m is the mass at the nucleus site and the indices on m, u and v have been dropped. The harmonic portion of the Hamiltonian (Equation (2-3)) may be written in terms of the normal coordinates. It would then be in the form of a sum of uncoupled harmonic oscillators of frequency $\omega_i^2 = A^{(2)}/m_i$. Thus in the harmonic approximation when deuterium is substituted for hydrogen, the U-center local mode frequency has a $\sqrt{2}$ isotope shift.

Creation and annihilation operators b and b^+ may be defined in terms of the normal coordinates. In this form the harmonic term of the Hamiltonian becomes

$$H^{har} = \tfrac{1}{2}\Sigma\, \hbar\omega_i (b_i^+ b_i + b_i b_i^+) \qquad (2\text{-}6)$$

where ω_i is the normal mode frequency. Solutions of this term for the cubic crystal are three degenerate local modes plus 3(N-1) optical modes and 3N acoustical modes where N is the number of unit cells. By a similar process, the terms of the anharmonic Hamiltonian may be written in the form

$$V^{(3)} = \frac{1}{3!} \Sigma\, \Sigma\, \Sigma C^{(3)}_{123} (b_1 + b_1^+)(b_2 + b_2^+)(b_3 + b_3^+) \qquad (2\text{-}7)$$

where the coupling constants are of the form

$$C^{(3)} = \left[\frac{\hbar}{2}\right]^{3/2} \frac{1}{\sqrt{\omega_1 \omega_2 \omega_3}} \Sigma\, \Sigma\, \Sigma A(3) \frac{1}{\sqrt{m_1 m_2 m_3}} v_1 v_2 v_3 \qquad (2\text{-}8)$$

Properties of hydrogen and deuterium U-centers will be compared later. It is hoped the form of the $C^{(n)}$ functions will explain the isotope effects seen in those properties that arise from the anharmonic terms in the potential.

Hanamura and Inui (13), following the method of Kubo (14), calculated a correlation function for the U-center problem. They showed that the expression for the absorption coefficient in terms of the correlation function could be expanded into a modified Lorentzian form. The width of the absorption curve at half-maximum (half-width Γ_α) may be written

$$\Gamma_\alpha = \frac{2\pi}{\hbar^2} \frac{< \{ [[a^+, H'(0)], H'(0)] a \} >}{2\bar{n}_\alpha + 1} . \qquad (2\text{-}9)$$

In this equation a and a^+ are operators for the local mode, $H'(0)$ is the $\omega = 0$ Fourier coefficient of H^{anhar} and $\bar{n}_\alpha$ is the average phonon number for the local mode. The curly brackets mean symmetrize,

$$\{AB\} = \tfrac{1}{2}(AB + BA). \qquad (2\text{-}10)$$

In this discussion when specific processes are described a and a^+ are used for operators which are restricted to local modes. Similarly ω_α is a local mode frequency and m_α is a U-center mass where the subscript α may be either hydrogen or deuterium. In equations where a's are used for local modes, b and b^+ refer to lattice modes.

Without considering any specific model for the potential, expand H^{anhar} and consider pertinent terms.

$$V^{(3)} = \frac{1}{3!}\sum\sum\sum_{123} C^{(3)}[(b_1 b_2 b_3 + b_1^+ b_2^+ b_3^+) \qquad (2\text{-}11a)$$

$$+3(b_1 b_2 b_3^+ + b_1^+ b_2^+ b_3)] \qquad (2\text{-}11b)$$

In this equation $3b_1 b_2 b_3^+$ represents $b_1^+ b_2 b_3 + b_1 b_2^+ b_3 + b_1 b_2 b_3^+$.

$$V^{(4)} = \frac{1}{4!}\sum\sum\sum\sum_{1234} C^{(4)}[(b_1 b_2 b_3 b_4 + b_1^+ b_2^+ b_3^+ b_4^+) \qquad (2\text{-}12a)$$

$$+ 4(b_1^+ b_2 b_3 b_4 + b_1 b_2^+ b_3^+ b_4^+) \qquad (2\text{-}12b)$$

$$+ 3(b_1^+ b_2^+ b_3 b_4 + b_1 b_2 b_3^+ b_4^+)] \qquad (2\text{-}12c)$$

$$V^{(5)} = \frac{1}{5!}\sum\sum\sum\sum\sum_{12345} C^{(5)}[(b_1 b_2 b_3 b_4 b_5 + b_1^+ b_2^+ b_3^+ b_4^+ b_5^+) \qquad (2\text{-}13a)$$

$$+ 5(b_1^+ b_2 b_3 b_4 b_5 + b_1 b_2^+ b_3^+ b_4^+ b_5^+) \qquad (2\text{-}13b)$$

$$+ 10(b_1^+ b_2^+ b_3 b_4 b_5 + b_1 b_2 b_3^+ b_4^+ b_5^+)] \qquad (2\text{-}13c)$$

Not all of the anharmonic terms have physical significance for this problem. In addition, some terms are significant only for specific frequency combinations. The terms important for a discussion of U-centers may be written:

(2-11b) $a^+ b_1 b_2 \delta(\omega_\alpha - \omega_1 - \omega_2)$ Decay of a local mode into two lattice modes. This is not energetically possible for any of the crystals under consideration.

$aa^+ b_1$ High frequency sideband

$aa^+ b_1^+$ Low frequency sideband

(2-12b) $a^+b_2b_3b_4\delta(\omega_\alpha-\omega_1-\omega_2-\omega_3)$ Decay of a local mode into three lattice modes. Since this is energetically possible for CsBr:D^- and CsI:D^- it would contribute to H'(0) in these cases.

$aa^+b_1b_2$ Two phonon sideband

(2-12c) $aa^+b_1b_2^+\delta(\omega_1-\omega_2)$ Decay through the modulation, Raman or scattering mechanism. This will contribute to H'(0) and will be discussed later.

$aa^+b_1b_2^+$ $(\omega_1\neq\omega_2)$ Two phonon difference sideband

$a_1a_1^+a_2a_2^+$ Broadening through interaction of one local mode with another. This is expected to be small since the modes are localized and the concentration of centers is low with respect to the spatial extent of each mode.

(2-13b) $a^+b_1b_2b_3b_4\delta(\omega_\alpha-\omega_1-\omega_2-\omega_3-\omega_4)$ Decay of a local mode into four lattice modes. This is energetically possible for all U-centers under discussion.

$aa^+b_1b_2b_3$ Three phonon sideband

(2-13c) $a^+b_1^+b_2b_3b_4\delta(\omega_\alpha+\omega_1-\omega_2-\omega_3-\omega_4)$ A decomposition process energetically possible for deuterium centers

$aa^+b_1b_2^+b_3^+$ $\omega_1=\omega_2+\omega_3$ Higher order scattering term If $\omega_1\neq\omega_2+\omega_3$ this will represent a higher order difference sideband.

Several decay mechanisms have been given which may contribute to H'(0). Fortunately, the contribution to the half-width Γ_α of each of these terms is additive. First consider the decomposition mechanisms. A fourth order term is energetically possible for the deuterium centers.

$$H'(0) = \frac{1}{3\cdot 2\cdot 1} \sum\sum\sum\sum_{\alpha 123} C^{(4)} (a b_1^+ b_2^+ b_3^+ + a^+ b_1 b_2 b_3) \qquad (2\text{-}14)$$

Inserting this in the equation for the half-width we find:

$$\Gamma_\alpha(T) = \frac{\pi}{18\hbar^2} \sum\sum\sum\sum_{\alpha 123} C^{(4)} (1+n_1+n_2+n_3+n_1n_2+n_1n_3+n_2n_3) \cdot$$

$$\cdot \delta(\omega_\alpha - \omega_1 - \omega_2 - \omega_3) \qquad (2\text{-}15)$$

These n's pertain to lattice modes and each one may be represented by a distribution

$$n_1 = \frac{1}{e^{\hbar\omega_1/kT} - 1} \quad . \qquad (2\text{-}16)$$

This expression may be simplified by considering Figures 4 and 5. The curves are one-phonon densities of states as calculated by Karo and Hardy using their DD(-) model. The frequencies marked on each figure are one third and one fourth the local mode frequencies as well as the low temperature (25°K) values of ω_{LO} and ω_{TO} measured by Vergnat et al. (15).[1]

[1] An additional determination of the LO frequencies in CsBr and CsI has become available recently (16). These values are about the same for CsI (91.5 cm^{-1} at 5°) and slightly lower for CsBr (115 cm^{-1}). It appears to be definite that Vergnat's values are an upper limit and that neither hydride U-center can decay into three lattice modes.

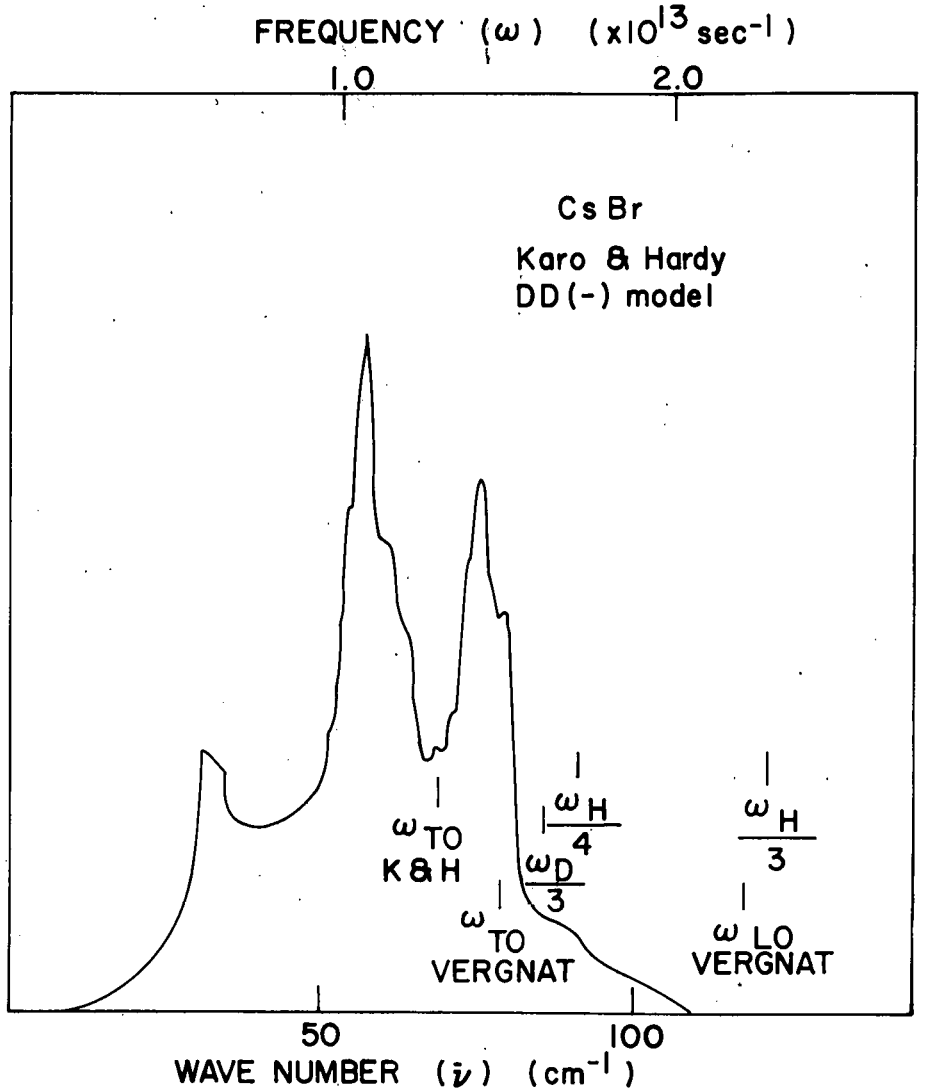

Figure 4. CsBr one-phonon density of states calculated by Karo and Hardy. Measured frequencies are marked.

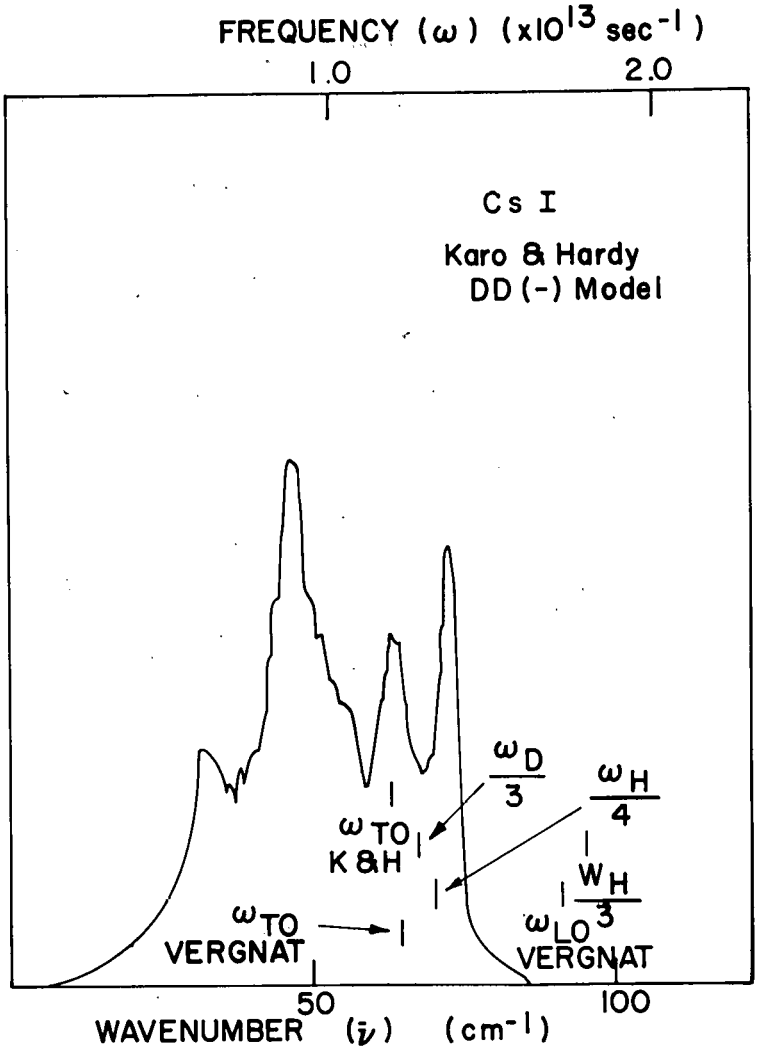

Figure 5. CsI one-phonon density of states calculated by Karo and Hardy. Measured frequencies are marked

For both CsBr and CsI, $1/3\omega_D$ is well into the optical band. If one of the ω_i lattice modes were in the acoustic band, one or both of the other modes would have to be near ω_{LO} where the density of states is low. It is reasonable, therefore, that the major contribution to Γ_D would come from lattice frequencies near $\omega_{avg} = 1/3\omega_D$. We may then write

$$\Gamma_D(T) = \frac{\pi}{18\hbar^2} \Sigma(C^{(4)})^2(1 + 3n_{avg} + 3n_{avg}^2) \qquad (2\text{-}17)$$

where

$$n_{avg} = \frac{1}{e^{\hbar\omega_D/3kT} - 1} . \qquad (2\text{-}18)$$

At low temperatures n_{avg} approaches zero so that

$$\Gamma_D(0) = \frac{\pi}{18\hbar^2} (C^{(4)})^2 = \frac{\text{Const.}}{(\omega_{avg}^{m_{latt}})^{3\omega_D m_D}} \qquad (2\text{-}19)$$

(See Equation (2-8)).

At high temperatures n_{avg} goes as T so that

$$\Gamma_D(T) \sim T^2$$

Following the same procedure, the temperature and isotope dependence of other terms may be determined. It is energetically possible for the hydrogen center to decay into four lattice modes. This mechanism will have a T^3 dependence at high temperature and will become constant at low temperatures.

There may also be a contribution to Γ_D from terms such as:

$$H'(0) = \frac{2}{4\cdot3\cdot2\cdot1} \sum_{\alpha 1234}\sum\sum\sum\sum C^{(5)}(ab_1b_2^+b_3^+b_4^+ + a^+b_1^+b_2b_3b_4) \delta(\omega_\alpha+\omega_1-\omega_2-\omega_3-\omega_4) \tag{2-20}$$

$$\Gamma_D(T) = \frac{\pi}{72\hbar^2} \Sigma(C^{(5)})^2(n_1+n_1n_2+n_1n_3+n_1n_4+n_1n_2n_4+n_1n_3n_4+ n_1n_2n_3-n_2n_3n_4). \tag{2-21}$$

This mechanism will also have a T^3 dependence at high temperature but the half-width will go to zero at low T. This is reasonable since it depends upon the existence of a thermally excited phonon.

There is also a contribution to the half-width from terms in H'(0) such as

$$H'(0) = \frac{1}{8} \sum_{\alpha 12}\sum\sum C^{(4)}(aa^+b_1b_2^+ + a^+ab_1^+b_2) \delta(\omega_1-\omega_2) \tag{2-22}$$

In this mechanism a lattice phonon is scattered at the local excitation. The scattered phonon has a different $\bar{k}$ than the incident one but the same energy. The local mode is given a fluctuating frequency and hence is broadened. It is possible for this method to be dominant over decay into three phonons, which has the same potential coefficient, because there is no restriction on the energy of the scattering phonons. It is necessary only to change $\bar{k}_i$ but not ω_i.

The temperature and isotope dependence may be determined in the same manner as for the decomposition mechanism.

$$\Gamma_\alpha(T) = \frac{\pi}{16\hbar^2} \Sigma(C^{(4)})^2(1 + n_1)n_2 \ , \qquad (2\text{-}23)$$

which goes as T^2 at high temperature and goes to zero at low temperatures. The isotope dependence from $C^{(4)}$ is $\Gamma_H/\Gamma_D = 2$. To say anything more requires a model which will define $C^{(4)}$.

Perhaps the simplest model is that of Elliott, Hayes, Jones, MacDonald and Sennett (17). Their work was concerned with the alkaline earth fluorides, but the method is general. In their determination of line width they assume the band modes are unperturbed by the defect and that the coupling is proportional to strain. They further assume a Debye model so that the strain is proportional to k (the wave vector) times the displacement. They further generalize to say that the strain is proportional to $\omega(k)/\omega_m$ where ω_m is the maximum frequency of the normal lattice. In this model the anharmonic term for decomposition into two lattice modes may be written

$$V^{(3)} = \Sigma\Sigma B' \frac{\hbar^2}{2mN\omega_m^2} \left(\frac{\hbar\omega_1\omega_2}{2m_\alpha\omega_\alpha}\right)^{\frac{1}{2}} \sum_{xyz} (a_x+a_x^+)(b_1+b_1^+)(b_1+b_1^+). \qquad (2\text{-}24)$$

Standard perturbation theory then gives the half-width

$$\Gamma_\alpha(T) = \frac{B^2\pi\hbar}{4m_\alpha\omega_\alpha m^2\omega_m^4} \sum_{1,2} \frac{1}{N^2} \omega_1\omega_2(1+n_1+n_2)\delta(\omega_\alpha-\omega_1-\omega_2). \qquad (2\text{-}25)$$

Using the Debye model for the lattice spectrum, the ω_i and n_i can be evaluated and the summation performed.

In this model, the appropriate potentials for the scattering mechanism are

$$V^{(3)} = \sum_{1} B \frac{\hbar^2}{2m_\alpha \omega_\alpha \omega_m} \left(\frac{\hbar\omega_1}{2mN}\right)^{\frac{1}{2}} \left[\sum_{xyz} (a_x + a_x^+)^2\right](b_1 + b_1^+). \quad (2\text{-}26)$$

$$V^{(4)} = \sum_{1,2} C \frac{\hbar^2 (\omega_1 \omega_2)^{\frac{1}{2}}}{4m_\alpha \omega_\alpha \omega^2 mN} \left[\sum_{xyz} (a_x + a_x^+)^2\right](b_1 + b_1^+)(b_2 + b_2^+) \quad (2\text{-}27)$$

The scattering mechanism may involve either $V^{(4)}$ in first order or $V^{(3)}$ in second order. The authors felt both terms were comparable in intensity so that the half-width may be written:

$$\Gamma_\alpha(T) = 2\pi \left(C - \frac{2B^2}{m_\alpha \omega_\alpha^2}\right)^2 \left(\frac{\hbar(2j+1)}{4m_\alpha \omega_\alpha m \omega_m^2}\right)^2 \sum_{1,2} \frac{1}{N^2} \omega_1^2 (1+n_1) n_2 \cdot \delta(\omega_1 - \omega_2) \quad (2\text{-}28)$$

where j is the local mode energy level number. As has been mentioned earlier the scattering mechanism thus goes as T^2 at high temperature and goes to zero as T goes to zero. For low T the sum may be evaluated, assuming the Debye model of the lattice, to obtain a T^7 dependence.

The form of $V^{(3)}$ given in Equation (2-26) also leads to single sidebands. Perturbation theory gives an intensity of the high energy sideband proportional to

$$\sum_{1} B^2 \frac{\hbar(n_1+1)\delta(\omega - \omega_1)}{2m_\alpha^2 m \omega_m^2 \omega_1 \omega_\alpha^2 N} . \quad (2\text{-}29)$$

The low energy sideband would have (n_1+1) replaced by n_1. At

low temperatures n_1 approaches zero and the summation becomes simpler. The intensity in this limit is proportional to $\rho(\omega)/\omega$. In the CaF_2 structure studied by Elliott, all lattice modes could contribute to the sideband (3). In the alkali halides $\rho(\omega)$ would represent only those states permitted by symmetry.

One very successful model for the NaCl lattice involving force constant changes has been developed in a series of papers by Timusk and Klein (18,12,19). The general structure, however, applies equally well to the CsCl lattice. The high frequency of the local mode relative to the normal lattice modes indicates that the mode is localized on the defect. For this reason, in the first approximation, only the defect and the nearest neighbors need be considered. A refinement by Gethins, Timusk and Woll (19) also includes the next nearest neighbors in the direction of motion of the defect. The improvement is important only in a detailed calculation.

The first step is to calculate the modes of the crystal in the harmonic approximation. The U-center is represented by a mass defect as well as a change in the effective force constant coupling the defect to the nearest neighbors. A formal solution for the perturbed lattice can be written in terms of a Green's function matrix of the perturbed lattice. The perturbed Green's function in turn may be written as an expansion in the perfect crystal Green's function and the

defect matrix. If the defect matrix is indeed localized, the dimension of the matrices will be small and the expansion solvable.

A set of trial configurations may be chosen from symmetry considerations and the matrix elements evaluated using wave functions calculated for the perfect lattice. As might be expected, the H^- ion vibrates in a triply degenerate odd parity mode along the coordinate axes with almost no motion of the adjacent lattice ions. (A truly static lattice gives a $\sqrt{2}$ isotope dependence, but on the other hand precludes any possibility of sidebands.) The result of this calculation in the harmonic approximation is the frequency of the local mode with only one adjustable parameter, the effective decrease in the force constant. The accuracy of this number is influenced, of course, by the quality of the calculation for the perfect crystal and the accuracy of the parameters used in that calculation.

The sidebands arise from the anharmonic terms of the Hamiltonian. As has been indicated before, the single sidebands are due to the third order anharmonicity. The simplest form of $V^{(3)}$ is

$$V^{(3)} = \tfrac{1}{2}BQ^2X. \qquad (2\text{-}30)$$

In this notation B is a constant, Q is the local mode dynamical coordinate and X is a combination of displacements of the neighbors. The local mode has odd parity while the perturbed

phonons, and hence X, are even. In this approximation for the anharmonicity, B can not depend on the defect mass, so the sidebands for H^- and D^- have the same strength. There is also a contribution to the absorption coefficient from the second order dipole moment. Lax and Burstein (20) discussed the physical origin of the second order dipole moment absorption. A vibrational mode may induce charge on an atom in addition to that normally present. A second vibrational mode simultaneously causes a vibration of this induced charge. This process produces an electric moment which can couple to the radiation field. All indications are that this term is small compared to the anharmonic coefficient B.

To the lowest order in the perturbation the high energy sideband is given by

$$1^+(\omega) = \frac{\hbar B^2}{8m^2\omega^3\omega_\alpha^2}\,\rho_X(\omega)(n_1+1) \qquad (2\text{-}31)$$

$\rho_X(\omega)$ is the perturbed density of states projected onto the coordinate X. Symmetry arguments were used in the introduction to determine which phonons would contribute to $\rho_X(\omega)$. The perturbed phonons may be calculated from the phonon spectra of the perfect crystal. The only adjustable parameter is the force constant change which may be determined by fitting the harmonic calculation to the experimental value of the local mode. The other important feature of this relation is that the sideband intensity is proportional to $\rho_X(\omega)/\omega^3$.

Bilz, Fritz and Strauch (21) have proposed a model which has many attractive features. Instead of changing the nearest neighbor force constant, they allowed the electron cloud of the H^- ion to polarize. A significant implication is that since the even-parity lattice phonons which contribute to the sidebands do not involve the defect, and the force constants have not been changed, the lattice phonons will not be perturbed. The isotope effect of the local mode frequency would be $\sqrt{2}$ because the isotopes would have the same polarizability.

The calculation is similar to that of Hanamura and Inui except that the Green's function formalism of Wehner (22) is used. The higher order dipole moment terms are explicitly retained as well as the anharmonic potential terms. This results in a high energy sideband of the form

$$I^+(\omega) \sim \omega \sum_i \left(\frac{3m_\alpha V^{(3)}(-\alpha,\alpha,i) 2\omega_\alpha}{\bar{\omega}_\alpha^2(\omega) - \omega^2} - M_2(\alpha,i) \right)^2 (n_i+n_\alpha+1) \cdot \delta(\omega_\alpha+\omega_i-\omega) \tag{2-32}$$

where

$$\bar{\omega}_\alpha^2(\omega) = \omega_\alpha^2 + 2\omega_\alpha \Delta_\alpha(\omega) \ . \tag{2-33}$$

M_1 and M_2 are the first and second order dipole moments and $\Delta_\alpha(\omega)$ is the shift function which in turn is a function of the anharmonic energy terms and higher order dipole moments. Consider the limiting case of $T = 0$ so that the occupation numbers n_i are zero. Further assume the eigenvectors of the

perturbed lattice are frequency independent so that the expansion coefficients may be written

$$M_1(\alpha) = \overline{M_1}/\sqrt{\omega_\alpha}$$

$$M_2(\alpha,i) = \overline{M_2}/\sqrt{\omega_\alpha \omega_i} \qquad (2\text{-}34)$$

$$V^{(3)}(\alpha,\alpha,i) = \bar{V}^{(3)}/\sqrt{\omega_\alpha^2 \omega_i}$$

where $\overline{M_1}$, $\overline{M_2}$ and $\bar{V}^{(3)}$ have no frequency dependence. (This is equivalent to assuming no frequency dependence in the $A^{(n)}$ or v_i in Equation (2-8).) Neglecting the shift function, the sideband absorption would be proportional to

$$\omega\left(\frac{3\bar{M}_1\bar{V}^{(3)}}{\omega_\alpha\omega_i(1 + \omega_i/2\omega_\alpha)} + \bar{M}_2\right)^2 \frac{1}{\omega_\alpha\omega_i}\,\rho(\omega_i) \qquad (2\text{-}35)$$

where $\rho(\omega_i)$ is the one phonon density of states at the lattice frequency ω_i. Thus the anharmonic absorption goes as $\rho(\omega_i)/\omega_i^3$ and the second order dipole absorption goes as $\rho(\omega_i)/\omega_i$. The approximations (2-34) above are not valid for the long wavelength acoustic modes. Instead, $\bar{M}_2$ and $\bar{V}^{(3)}$ are proportional to ω_i. Therefore for low k the sidebands are proportional to $\rho(\omega_i)/\omega_i$ if the only contribution is from the anharmonic term $V^{(3)}$.

An exact expression for the shift function is extremely complex. Bilz *et al.* discuss the low order terms which they feel are important. These terms all arise from the third order anharmonicity except for one term which is the main

higher order contribution from the fourth order anharmonicity. Therefore they all vary linearly with T at high T and go to a constant at low T. $V^{(3)}(\alpha,-\alpha,j)V^{(3)}(-j,i,-i)$ and $|V^{(3)}(\alpha,i,j)|^2$ produce shifts of opposite sign and approximately equal magnitude. They are also small since there is a term in the denominator which goes as the difference between the local mode frequency and the maximum normal lattice frequency. Similarly, shifts due to potential terms which give rise to sum and difference sidebands are nearly equal in magnitude but different in sign and cancel. There is a negative shift due to thermal expansion of the lattice. Thermal expansion, however, is due to anharmonicity of the lattice in general, not just the defect, and is not explicitly included in this theory. The term which Bilz feels is significant is the main term due to the fourth order anharmonicity--$V^{(4)}(\alpha,-\alpha,i,-i)$. This is a positive shift linear in T.

Elliott *et al.* derive a simple expression for peak shift from this anharmonic term. Averaging Equation (2-27) over the band modes (cross terms in b_1 and b_2 go to zero) (17)

$$V^{(4)} = \sum_{1} C \frac{\hbar^2 \omega_1}{4 m_\alpha \omega_\alpha \omega_m^2 mN} \left(\sum_x (a_x^+ a_x + a_x^+ a_x)\right)(b_1^+ b_1 + b_1^+ b_1). \qquad (2\text{-}36)$$

Compare this to the harmonic oscillator Hamiltonian

$$\tfrac{1}{2}\hbar\omega_\alpha \sum_x (a_x a_x^+ + a_x^+ a_x).$$

The effective shift is

$$\frac{\Delta\omega_\alpha}{\omega_\alpha} = \frac{C}{m_\alpha \omega_\alpha^2 m \omega_m^2} \left(\frac{1}{N} \sum_l \hbar\omega_l (n_l + \tfrac{1}{2}) \right). \qquad (2\text{-}37)$$

The term in parentheses is the mean vibrational energy which goes as T at high temperature. The terms $m_\alpha \omega_\alpha^2$, however, result in a zero isotope dependence.

EXPERIMENTAL

The samples used were purchased from Harshaw Chemical Company. Pieces approximately $\frac{1}{2}x\frac{1}{2}x\frac{1}{4}$" were additively colored with potassium by the van Doorn (23) method to produce F-centers. The blocks were then cut into slices approximately 2 mm thick and polished. F-centers were converted into U-centers by heating the crystal sealed in a stainless steel bomb in a hydrogen (1400 psi) or deuterium (600 psi) atmosphere. CsBr and CsI were held at 425°C for 3 hours and 1 hour respectively. At the end of this time the bomb was cooled to room temperature in about ten minutes. Samples required repolishing but an effort was made to keep this to a minimum as the U-center concentration was heaviest near the surface. Concentration adjustments were made by varying the F-center concentration.

The electronic absorption was measured in the ultraviolet at room temperature to get an indication of concentration even though the optical density was too great at the concentrations used to get a quantitative measure.

At one time Mitra and Brada (9) reported that cesium halide U-centers were unstable at room temperature. This does not appear to be the case. Samples over a year old were measured and no changes could be detected. In addition, samples were heated to 500°C for ten minutes and quenched. Again, this had no measureable effect. This would indicate

that high concentrations of U-centers could be obtained by repeating the additive coloration and hydrogenation. However, surface damage from the potassium removed the portion of the crystal that contained the bulk of the centers produced in the previous cycle.

The sample cryostat used has been described by Lott (24). A sample and a reference or blank were mounted side by side on the tail of a liquid helium optical cryostat. The entire cryostat slid on teflon rods perpendicular to the beam so that either crystal could be put into the beam. The space around the sample could be sealed off by liquid helium temperature exchange gas windows so that He gas could be used to help cool the samples. In this work polyethylene exchange gas windows were used. Twenty micron thick polyethylene film was sandwiched between broad rings of polished brass held together with small machine screws around the perimeter. A film of vacuum grease on both sides of the polyethylene made the vacuum seal. Thicker windows were only occasionally successful. They often shattered, apparently a result of internal strains, when cooled. As gas pressures required were very small (25 microns of Hg maximum), in general if the windows survived cooling they had more than adequate strength.

Samples for main peak measurements were mounted in the exchange gas space with poor thermal contact to the copper tail. The temperature was measured with a Au-0.02% Fe vs. Cu

thermocouple sealed with vacuum grease in a number 80 hole drilled in the sample. The EMF was monitored with a digital voltmeter during the scan. With no exchange gas (pressure less than 10^{-5} mm Hg) the sample temperature was about $35^{\circ}K$ when the tail was at liquid helium temperature. A minimum temperature of 6° could be reached by using exchange gas. Any temperature between these limits could be obtained by adjusting the gas pressure. Even with no further temperature control the sample temperature was stable for the duration of a scan. Measurements above 35° were made as the sample warmed up after the He was gone. With a good vacuum in the exchange gas space it took several hours to reach 80° and thus temperature drift during a scan was not a significant problem.

Two different spectrometers were used for the infrared measurements. In measuring the main peak absorption the primary considerations were high resolution and wavelength stability. The monochromator used was a single-pass grating Perkin-Elmer model 98G. The detector was a Zn:Ge doped detector for all except the $CsI:D^{-}$ at fifty microns, where a thermocouple was used. Order sorting was done with bandpass filters after the exit slit instead of the foreprism normally used. When necessary a reststrahl filter was also used. In general stray light was not a problem. The doped detector has a peak sensitivity near 35 microns and drops off rapidly

at longer wavelengths and more slowly as the wavelength approaches the globar peak at 2.5 microns. In these measurements a significant method of determining stray light is to look at a sample with a high concentration of centers so that the peak absorption should be extremely high. The only measurement for which stray light was a problem was the CsI:D^- main band at about 50 microns. In this wavelength region it was necessary to use the thermocouple (which was sensitive to the globar peak) and the least efficient of the bandpass filters. To compound the problem, the region of interest was near the blaze of the grating so that higher order light was stronger than usual. An approximate correction was made by using KBr as a shutter and scanning the range to determine a baseline. KBr has a long wavelength transmission limit of 40 microns.

Rotation lines of water vapor were used to calibrate the spectrometer. The energies used were those determined by Randall *et al.* (25). The resolution of this spectrometer (typically 0.6 to 0.7 cm^{-1}) was comparable to Randall's facilitating easy identification of the structure. The measured points were fit to an n'th order polynomial by a least squares computer routine. The order of the polynomial was chosen for best fit.

A digital data system eliminated the necessity of reading strip charts. The doped detector was used at 4.2°K where it

had a resistance of 12 megohms. It was used with a 2.5 megohm load resistor and a 30 volt bias battery. The AC signal was synchronously detected and amplified. The output of the amplifier went to an integrating digital voltmeter and was also recorded on a strip chart for monitoring. A control unit determined the sampling rate and synchronized the sampling times to the wavelength drive. A digital recorder automatically printed out the voltmeter reading along with the appropriate monochromator drum number. The drum number could be converted to energy with the calibration polynomial.

The sample and a blank of the same material and equal thickness were scanned alternately. This minimized the effect of slow variations in beam intensity. The ratio of the two signals gave the absorption of the U-centers without the contribution from the host lattice and reflectivity losses.[1] Transmission ($T = I/I_o$) and optical density ($OD = \log_{10}(I_o/I)$) were then calculated as a function of energy.

If the width of an absorption band is within an order of magnitude of the bandpass, the measured absorption will be artificially broadened. If the true shape of the band and the shape of the bandpass function are known, they may be convolved and the measured shape and width determined. In general, however, determination of the true shape is the goal

---

[1]With a low concentration of defects the index of refraction should not be changed significantly.

of the measurement. The problem in the case of the U-center has several simplifying features. The local mode is well isolated in energy from the crystal absorption and it is a single peak (actually three degenerate modes). Also, from the discussion in the appendix, the bandpass function is nearly triangular, with a width that may be calculated reasonably accurately. Ramsay (26) pointed out that a Lorentzian convolved with a triangle was nearly Lorentzian. That is, either the main portion of the peak or the wings could be fit by a Lorentzian, but not both by the same Lorentzian. The measured CsBr:H^- and CsBr:D^- spectra could be fit to a Lorentzian from $(OD)_{max}$ to $1/10(OD)_{max}$. For this reason, the correction tables compiled by Ramsay for Lorentzians were used for CsBr in the region in which they applied. The CsI case will be discussed later.

The sideband spectra were measured on a double-pass prism monochromator (Perkin-Elmer model 99) with a thermocouple detector. This combination has a large wavelength range and good signal stability, but wavelength stability and resolution are relatively poor. Water vapor was also used for the calibration of this monochromator. Many of the lines are not resolved and the energy of the combined absorption maximum must be determined. Mills et al. (27) and Downie et al. (28) have published the appropriate energy values for calibrating lower resolution monochromators such as this one. As in the

case of the grating monochromator, the calibration was fit to a polynomial. The dispersion of prisms, especially a CsBr prism, is temperature sensitive. The wavelength drive is linear to the extent that if the correction to the drum number could be determined at one wavelength it could be applied to all drum settings. For this reason an analytical expression for the wavelength as a function of drum number was valuable for determining the proper calibration of a given scan.

For the sideband measurements the sample and reference blank were mounted on the cryostat tail using wire clips and a film of Apiezon N grease. No exchange gas windows were used because of interference effects in the film. The temperature was monitored in the same manner as for the main peak measurements.

Because the sideband absorption was so small, measurements were made point by point. The output of the synchronous amplifier was fed into a digital voltmeter and integrated for ten second periods. The signal was monitored for several periods for each reading as a check on stability. With this method the transmission measurements were reproducible to within about 0.2%. This is, however, still a large error in absorption. The data were taken at constant slit width because the concentration of centers was nonuniform. For this reason the resolution in some portions of the spectrum was very poor.

DISCUSSION

U-centers in CsBr and CsI have somewhat different properties and will be discussed separately. Representative absorption curves for the CsBr:H^- and CsBr:D^- local modes are given in Figures 6 and 7. They are generally symmetric, have a pronounced temperature-dependent width and have a slight shift of peak energy with temperature. The apparent large change in integrated absorption as a function of temperature is a manifestation of finite bandpass and will be discussed later. Most features of the CsBr U-center fit the models that have been proposed.

Figure 8 shows the half-width of CsBr:H^- as a function of T^2. In the range where it was possible (25° and above) the half-width has been corrected using the tables compiled by Ramsay (26). These measurements show a T^2 dependence up to 70°. Earlier work by Bauer (8) shows the T^2 dependence extending to 175°. The corrections can not be applied below 25° as the measured width is too narrow. An extrapolation of the T^2 line shows the half-width going to zero near 12°. To examine this region, the inset shows the half-width of the measured transmission plotted as a function of T^2. This shows the absorption becomes extremely narrow but finite and apparently constant by $8^\circ K$.

Figure 9 is a similar plot for CsBr:D^-. The D^- center is in general narrower and bandpass corrections can not be

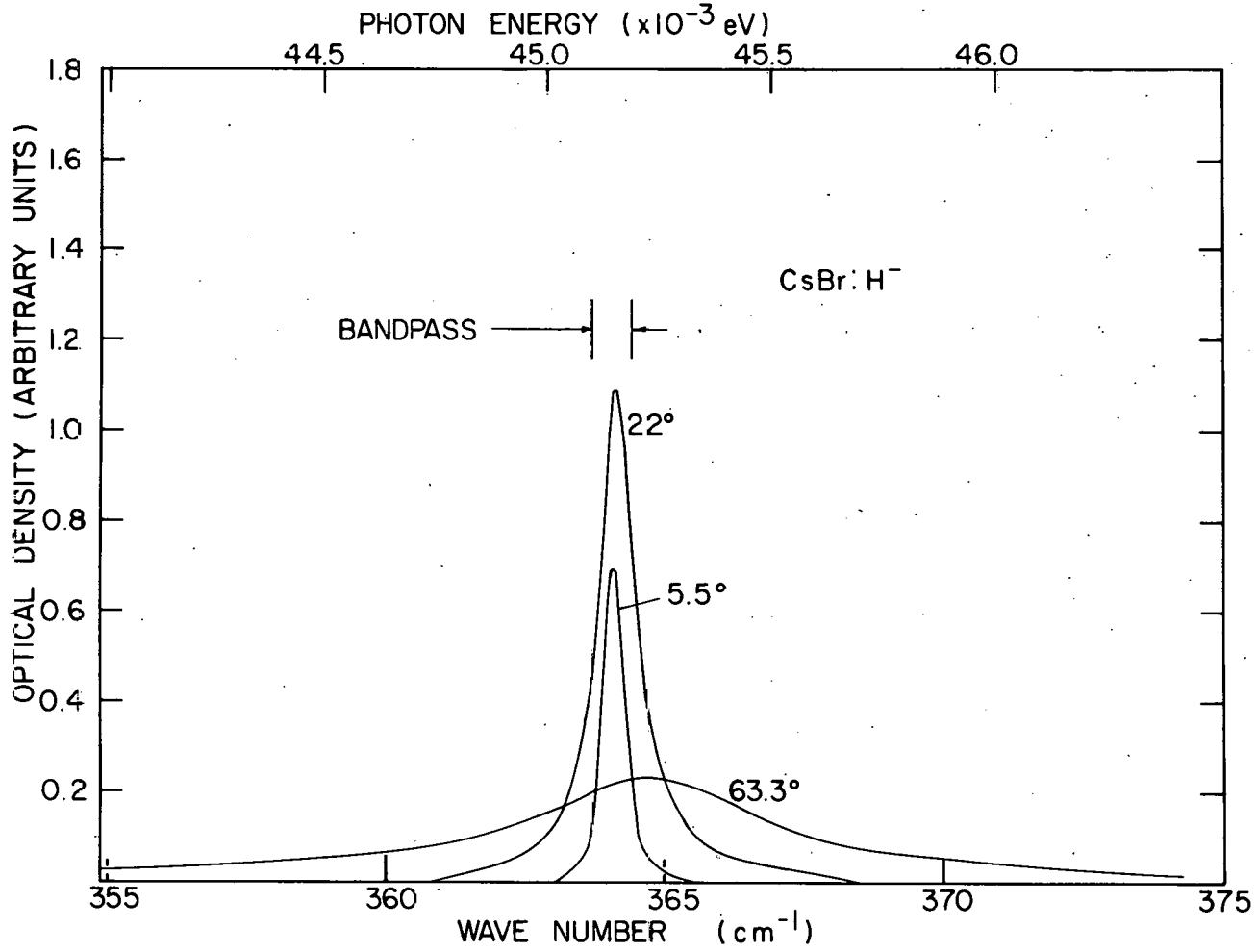

Figure 6. Examples of main peak absorptions due to CsBr hydrogen U-centers

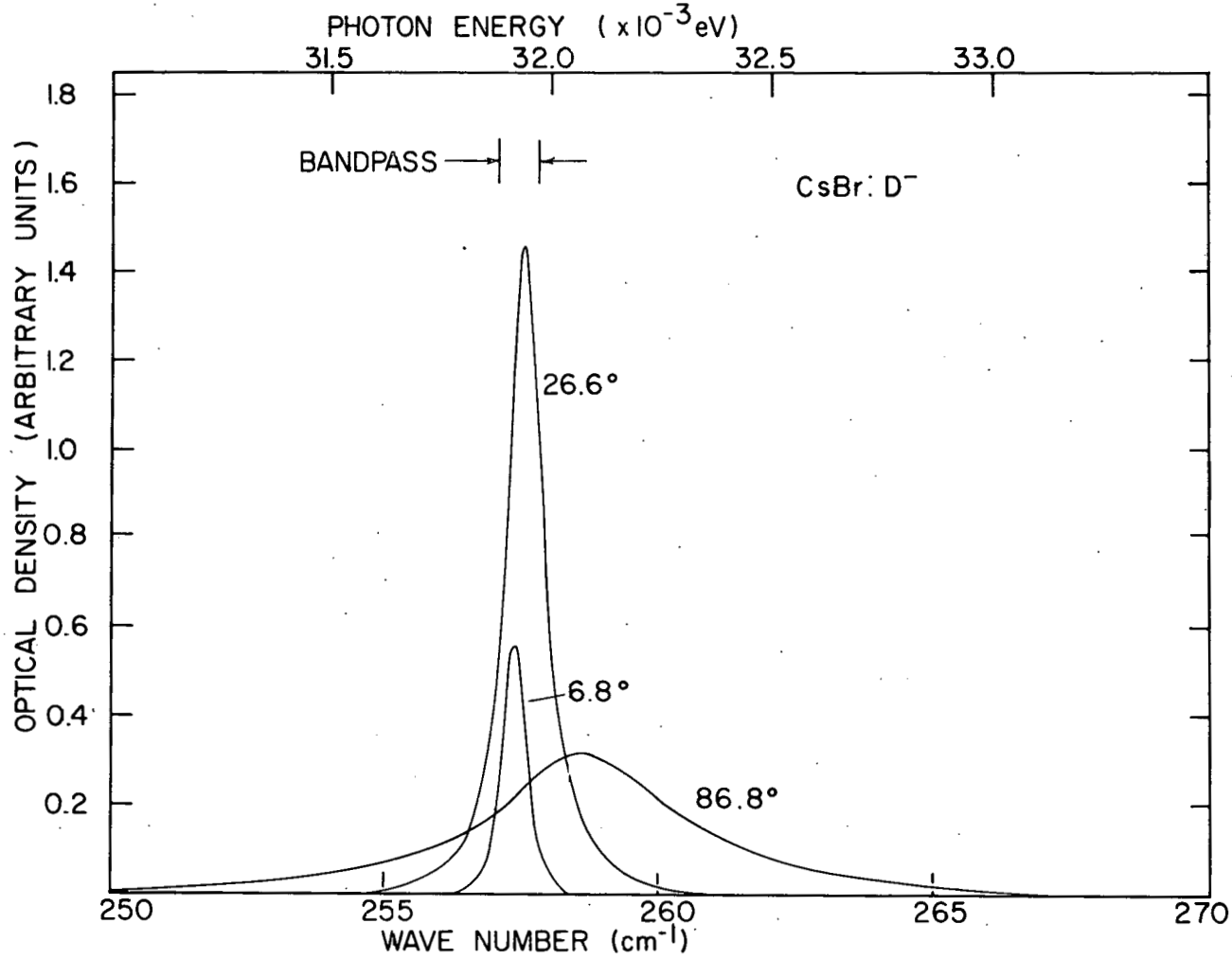

Figure 7. Examples of main peak absorptions due to CsBr deuterium U-centers

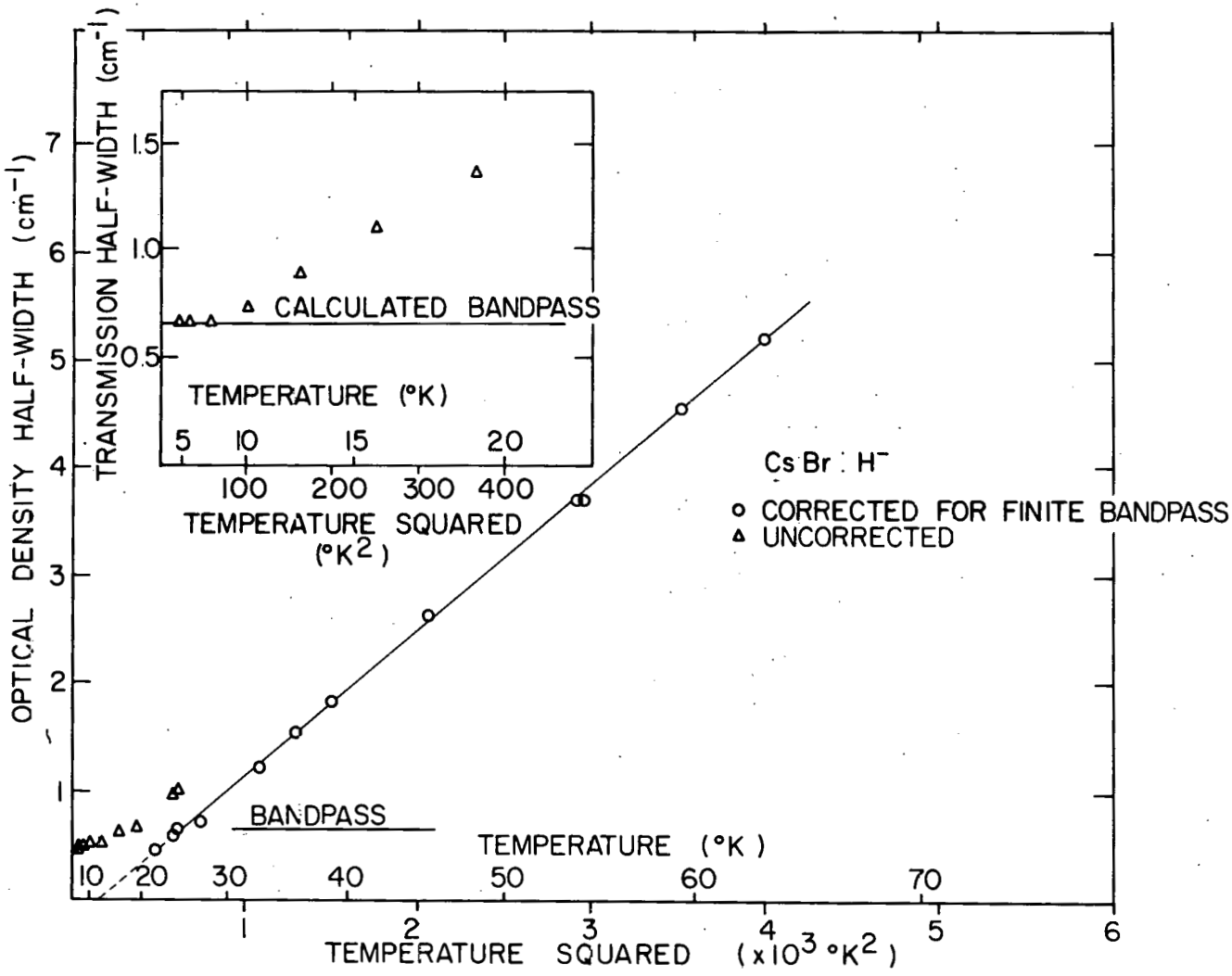

Figure 8. Half-width of CsBr hydrogen U-center as a function of temperature squared

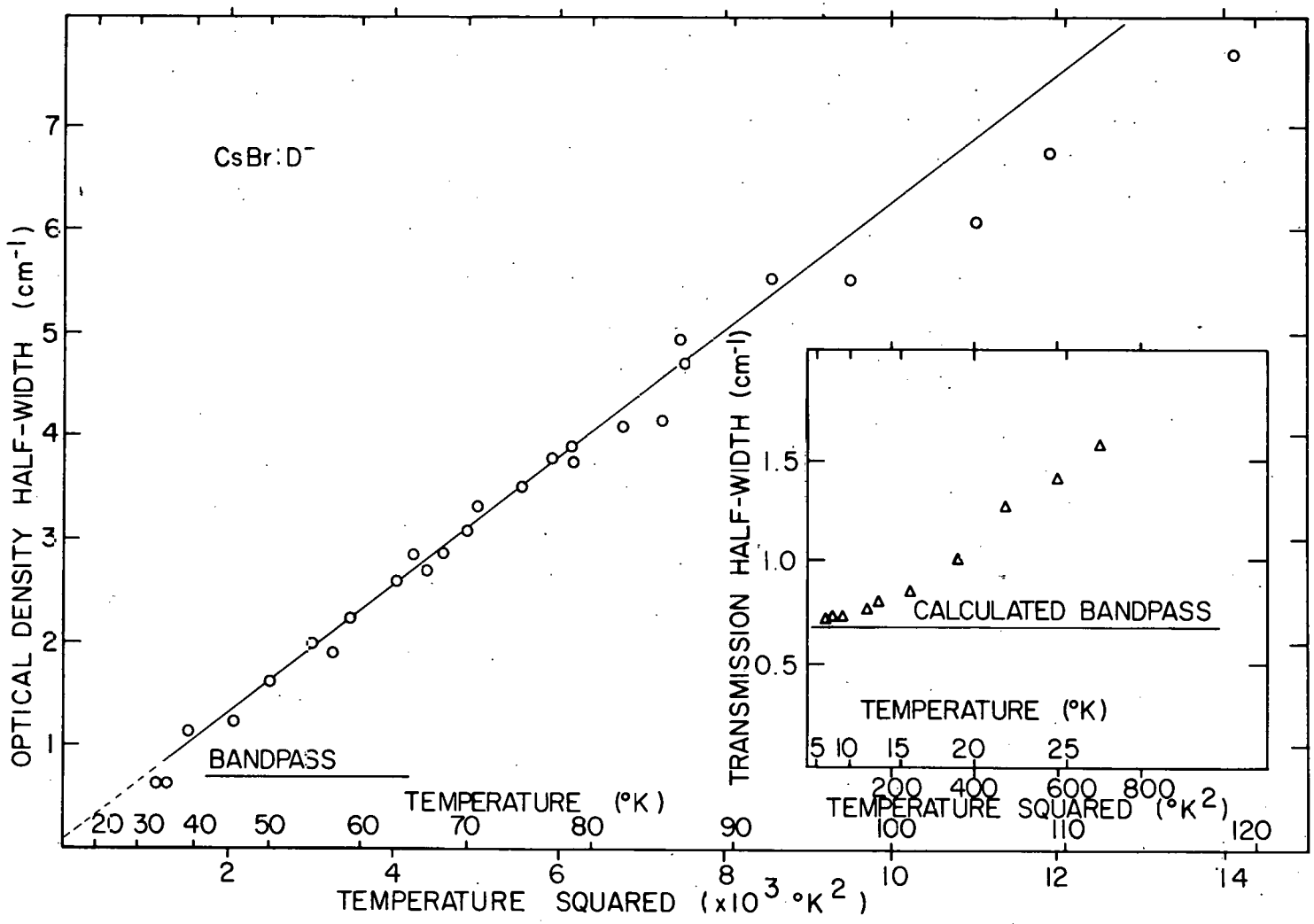

Figure 9. Half-width of CsBr deuterium U-center as a function of temperature squared

applied below 40°. The temperature dependence is T^2 from 40° to 95° where it becomes somewhat less. At low temperature the transmission half-width approaches a constant value.

Neglecting for the moment the deviation of the CsBr Γ_D temperature dependence from T^2 at high temperatures, the half-widths of several U-centers (extrapolated to low temperatures) are plotted as a function of T^2 in Figure 10. The half-width of KBr:H^- is given for comparison. (KBr:H^- is the most extensively studied of the NaCl structure U-centers. The data given were measured on the prism monochromator as a check on the equipment. There is a wide range of values in the literature (See Reference 11 for a summary.), presumably because of a high sensitivity to internal strain and impurities (29). The widths measured are among the higher values reported.)

The decomposition process for the H^- center would require four lattice phonons leading to a T^3 dependence at high temperature and going to a constant value at T = 0 determined in part by the magnitude of the fifth order anharmonic term. The D^- local mode could decay into three lattice phonons through the fourth order term. The temperature dependence for this would be T^2, again going to a constant at T = 0. The actual mechanism appears to be the scattering or modulation term which goes as T^2 for both centers. The relative half-widths come from the isotope masses and local mode frequencies, giving

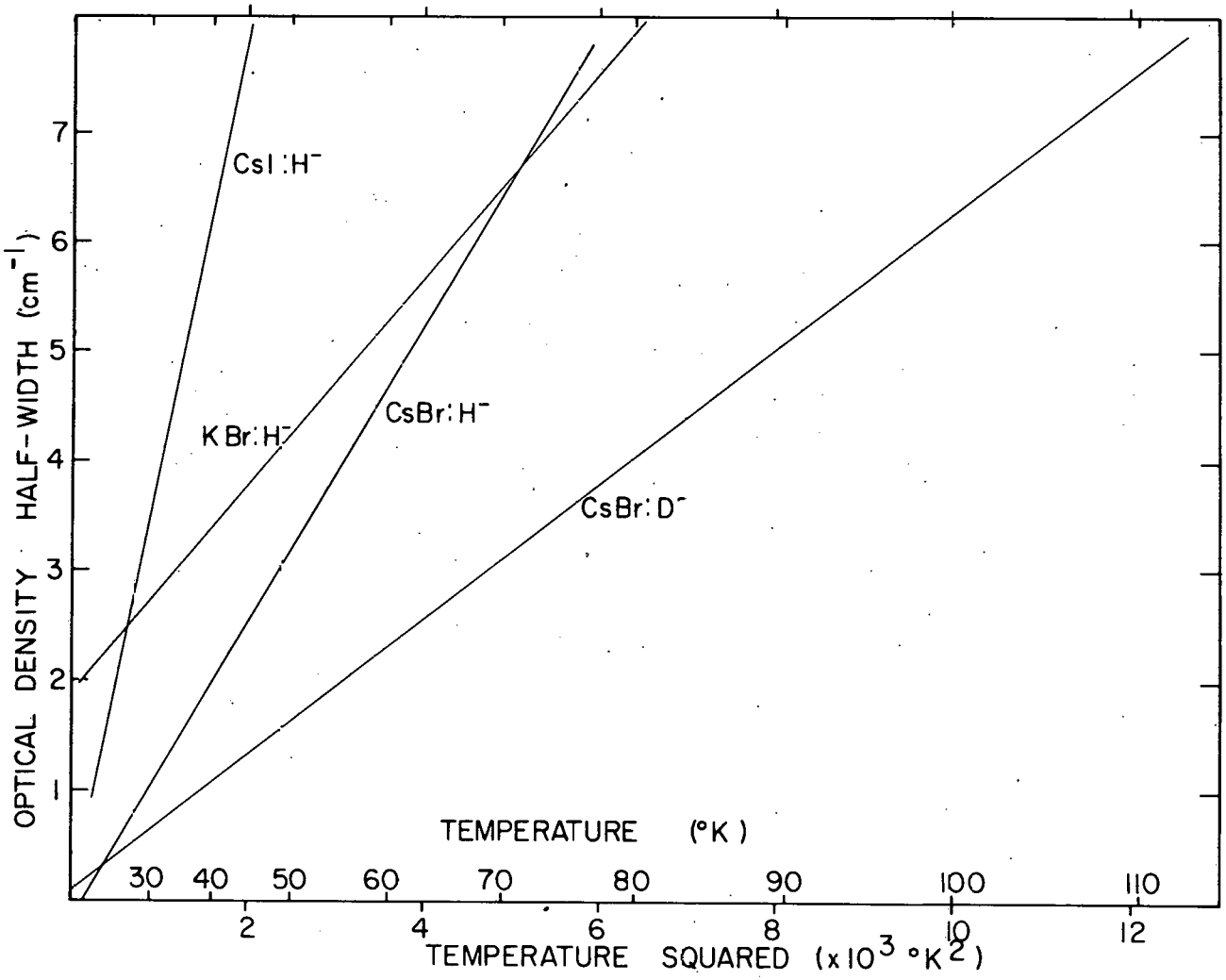

Figure 10. Half-widths of several U-centers as a function of temperature squared

a ratio $\Gamma_H/\Gamma_D = 2$ as measured. At low temperatures the modulation term goes to zero and the relatively weak decomposition terms take over. That the Γ_D term is larger in this limit is an indication that the fourth order anharmonic term is larger than the fifth. Also, the one-phonon density of states is larger at $\omega_{D/3}$ than $\omega_{H/4}$. Ivanov et al. (29) have shown that a slight admixture of the two mechanisms can maintain a T^2 dependence to quite low temperatures.

Figures 11 and 12 show the peak energy as a function of temperature. Each approaches a constant value at low temperature; 31.918×10^{-3} eV for CsBr:D^- and 45.146×10^{-3} eV for CsBr:H^-. The ratio is 1.414, the square root of two within the limits of calibration. This would support an essentially static lattice model, or a model such as that of Bilz et al. in which the H^- polarizability rather than a force constant change is the main feature (21).

Both U-centers show a positive energy shift with temperature. Again neglecting the high temperature data for D^-,

$$\Delta_H = 1.79 \times 10^{-6} \text{ eV/}^\circ\text{K} \quad (1.44 \times 10^{-2} \text{ cm}^{-1}/^\circ\text{K})$$

$$\Delta_D = 2.64 \times 10^{-6} \text{ eV/}^\circ\text{K} \quad (2.13 \times 10^{-2} \text{ cm}^{-1}/^\circ\text{K})$$

The ratio is near the square root of two.

$$\Delta_D/\Delta_H = 1.48$$

After normalization by the local mode energy, the ratio is 2:1.

Bilz et al. indicated that the shift associated with the

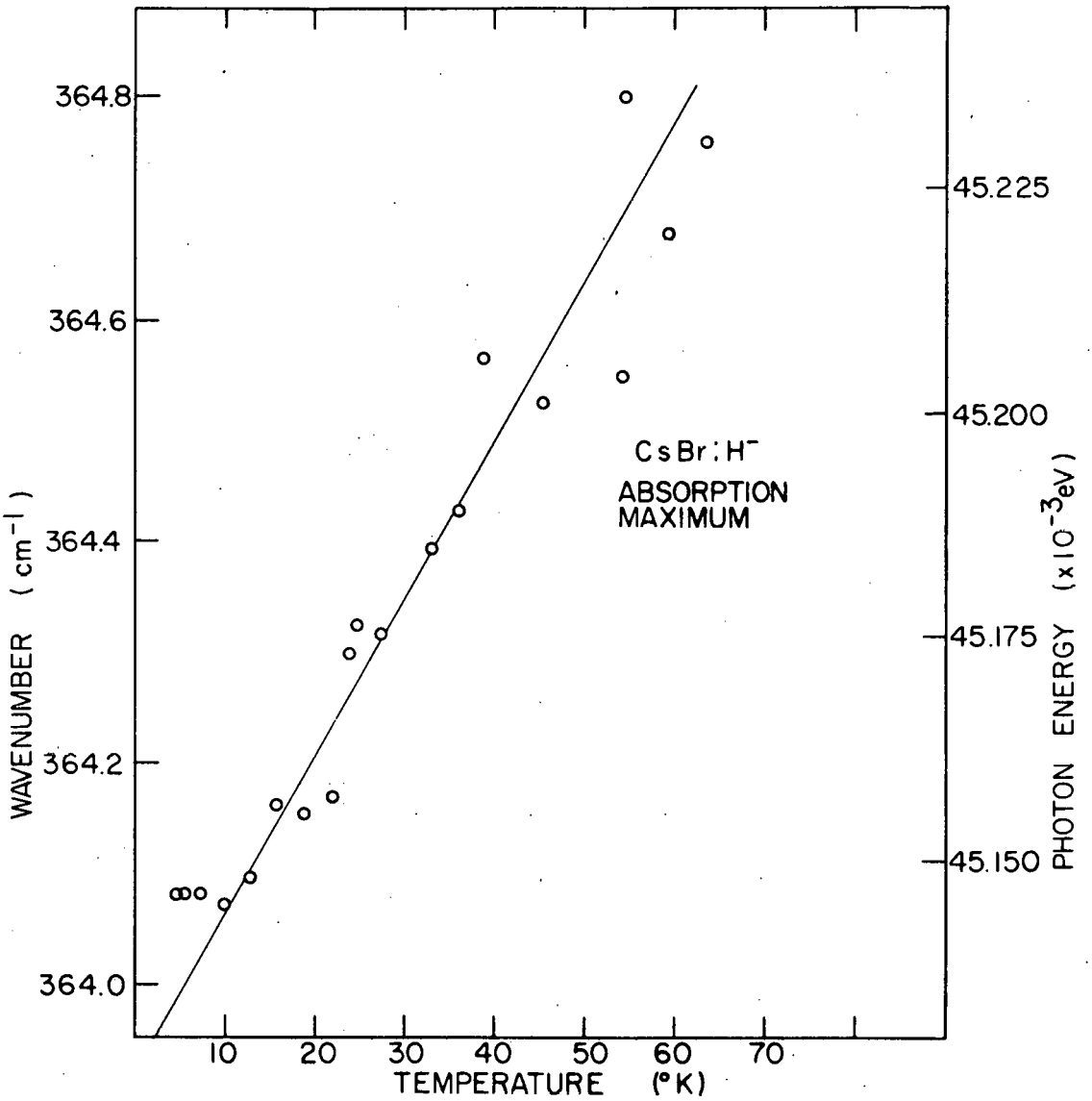

Figure 11. Shift of the CsBr hydrogen U-center as a function of temperature

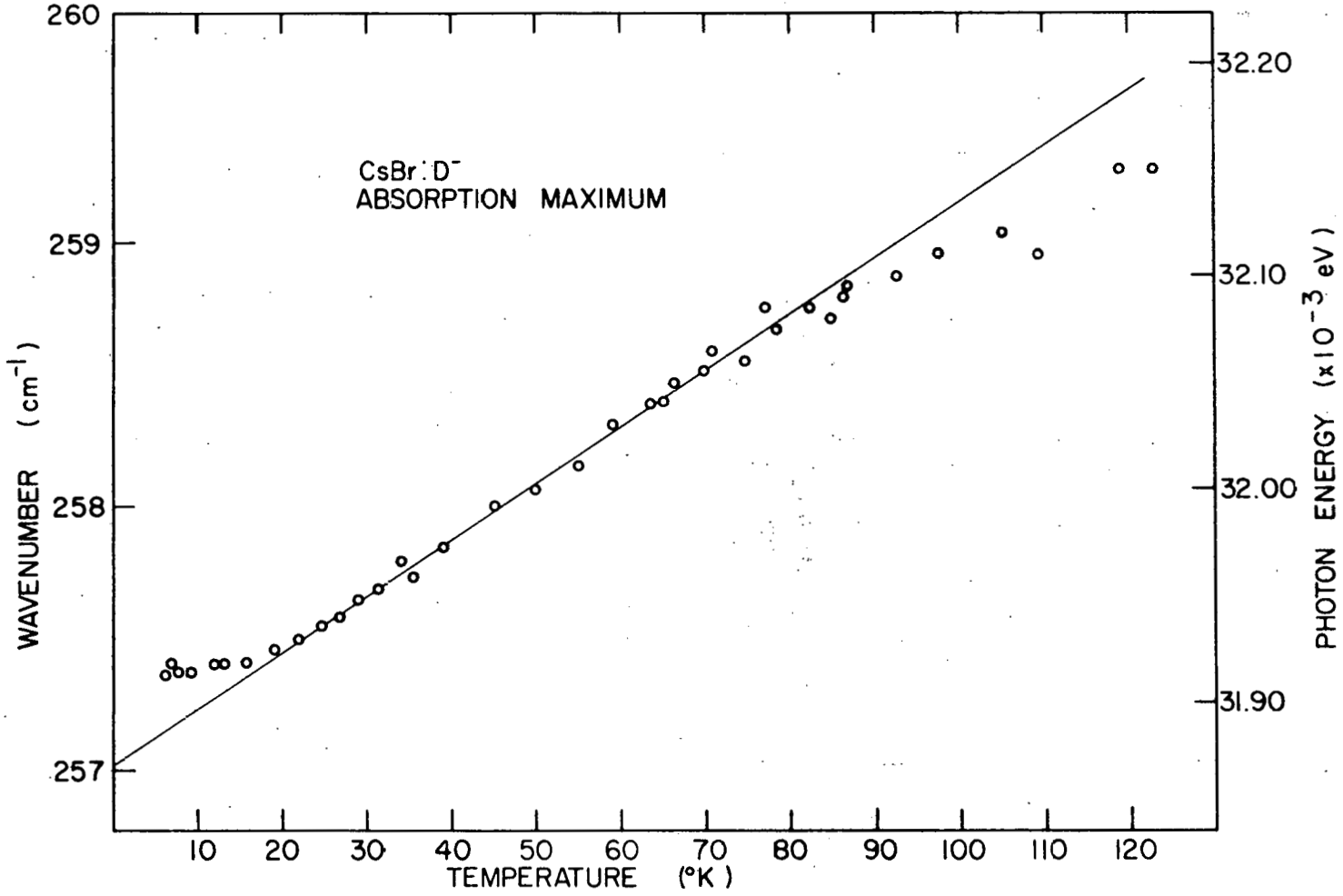

Figure 12. Shift of the CsBr deuterium U-center as a function of temperature

$V^{(4)}$ term should be larger for the deuterium center than for the hydrogen. The justification given for KBr was that $\omega_D < 2\omega_m < \omega_H$. However, in their equation for the peak shift the third order anharmonic terms have a frequency difference denominator, but the $V^{(4)}$ term does not. This form is in agreement with other authors. In this term, the local mode appears twice in $V^{(4)}$. Since the product $\omega_\alpha m_\alpha$ would then appear in the denominator of the potential, the isotope dependence from this source would be a deuterium shift smaller by $\sqrt{2}$ -- the opposite of experiment. It must be concluded that the $V^{(4)}$ term in the shift function as described by Bilz et al. will not account for the experimentally measured isotope effect. It is possible that one of the $V^{(3)}$ terms which does have a frequency difference denominator is responsible for the shift. More likely, it will require a more comprehensive model of the lattice and defect to properly account for such things as thermal expansion.

The temperature dependence of both the half-width and the peak shift of CsBr:D^- begin to deviate from a straight line at higher temperatures (about 90^o). The dominant term in the half-width is $V^{(4)}$ while the peak shift is due, at least in part, to $V^{(3)}$ or $V^{(4)}$. The deviations could be explained consistently by a weakening of the fourth order anharmonic potential at higher temperatures. Lowndes has looked at a related problem. He has resolved the temperature

and pressure shift of the longitudinal-optical frequency of CsBr into two temperature-dependent terms--that due to thermal expansion, and that due to a change in the phonon self-energy term. The form of the latter shift function is the same as for the local mode. The difference is that Lowndes is concerned with the anharmonicity of the perfect lattice potential not the defect potential. He finds that either the $V^{(4)}$ term increases significantly with temperature or the cubic term decreases. He also finds the shift due to thermal expansion is still small at 80^{o} but increases greatly by 200^{o}. These results would indicate that the most probable source of the relative decrease in the shift function is thermal expansion.

In Figures 6 and 7 it appears that the integrated area of the absorption curve decreases greatly at low temperature. These curves, however, have not been corrected for instrumental effects. It is generally assumed that the integrated area of an absorption curve is independent of instrumental resolution. This is not true in the realm of very narrow absorption lines (true half-width less than the bandpass). In the limit of a delta function absorption coefficient, no energy is absorbed (30). Calculating the convolutions of increasingly narrow Lorentzians with a triangular bandpass function has shown that the apparent reduction in area at low temperatures (e.g. Bauer (8)) is due to narrow line-

widths. Very accurate measurements of integrated area are difficult because of baseline uncertainties. There is no reason to believe, however, that the strength of the CsBr:H^- absorption is temperature dependent.

The sideband spectra of the CsBr U-centers are given in Figure 13. In comparison to most NaCl structure U-centers they are extremely weak. This is consistent with weak coupling to the lattice and a $\sqrt{2}$ isotope shift of the local mode. One interesting feature is that the high and low energy sidebands are not exactly symmetric about the local mode. This is the effect of a nonnegligible shift function.

There is an extra peak in the low energy sideband at $\omega_H - \omega = 1.42 \times 10^{13}$ sec^{-1} (35.8×10^{-3} eV). The peak is weak, but it appears in all samples with a sufficiently high concentration of U-centers. The shape and width of the peak at 33^o are almost entirely that of the bandpass function. Corrected, it shows typical local mode behavior--very narrow and very temperature dependent. The peak's position is consistent with a U-center having a light impurity on an adjacent Cs site. This would perturb all three modes equally since the impurity is in a (111) direction and the H^- vibrations are in the (100) directions. The degeneracy would be maintained. A smaller atom such as rubidium or potassium would provide a weaker coupling and hence lower frequency vibration. Either impurity is possible since rubidium is a common impurity in

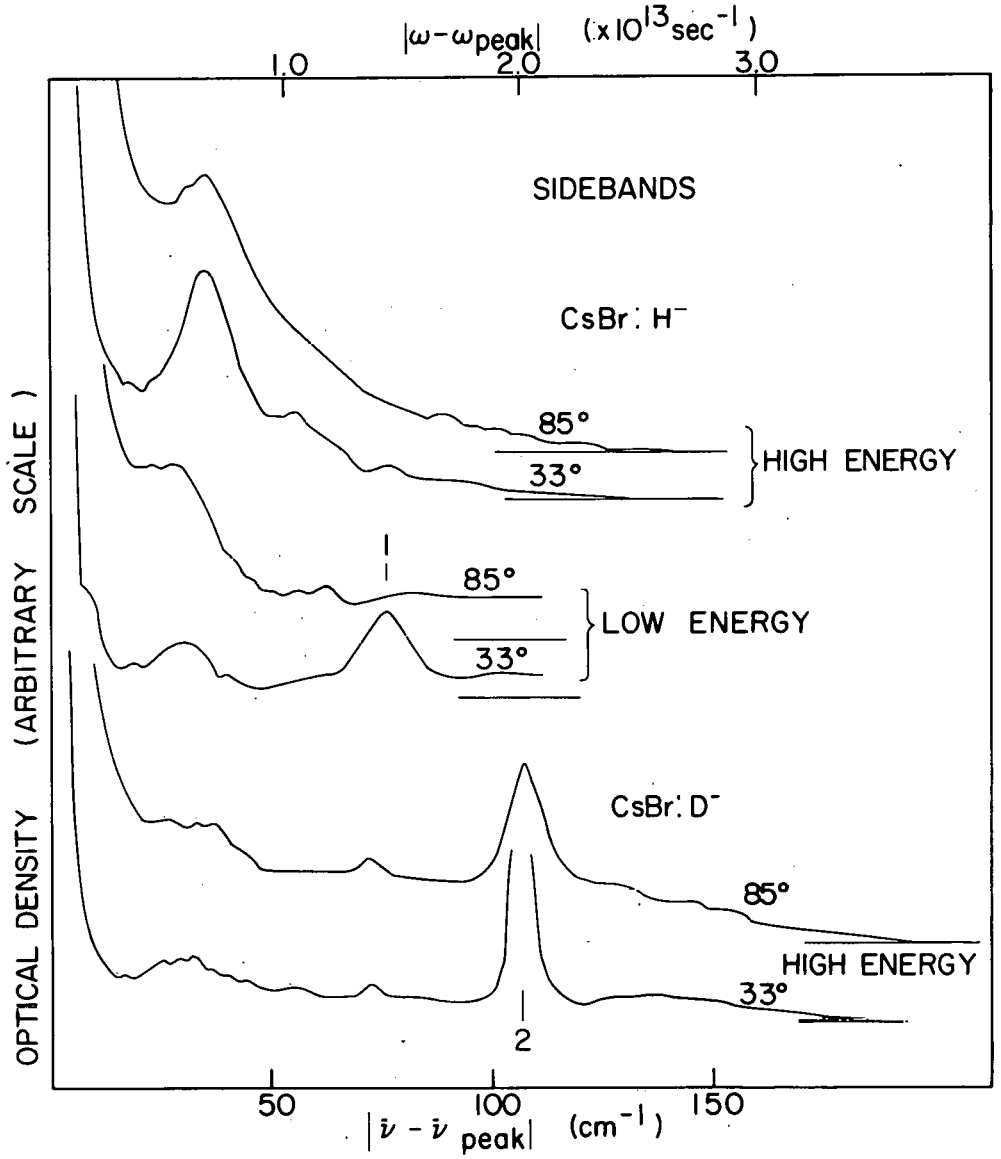

Figure 13. Sidebands of the CsBr U-center. The absorptions at the points marked (1) and (2) are not due to sidebands. See the text for details

cesium and the crystals were additively colored with potassium. The mode is not consistent with an adjacent halogen impurity such as a second H^- ion. This would split the local mode into a singlet and doublet. A second mode in the sideband spectrum is not seen, at least below 40 microns. The other possibility is an interstitial. This, however, would produce a shift to higher energy. The extra peak in the D^- sideband (2) is due to hydrogen impurity in the deuterium.

Figure 14 shows the high energy, low temperature H^- sideband with an ω^3 weighting factor. According to Klein this should be proportional to the perturbed one-phonon density of states. The symmetry requirements on the sidebands were discussed in the introduction. Karo and Hardy's DD(-) model one-phonon density of states is superimposed on Figure 14 with the most significant permitted phonons indicated by short vertical lines. The agreement is remarkably good. Both Elliott *et al.* (17) and Bilz *et al.* (21) point out that the proper weighting factor at low frequency is ω not ω^3. This will have the effect of moving the lowest measured peak to lower frequency, improving agreement with the calculated curve. The fact that it is still at too high a frequency may be an indication that there is some perturbation of the lattice phonons. The permitted phonons at that frequency are TA phonons at Σ, the point halfway to the zone edge in the (110) direction.

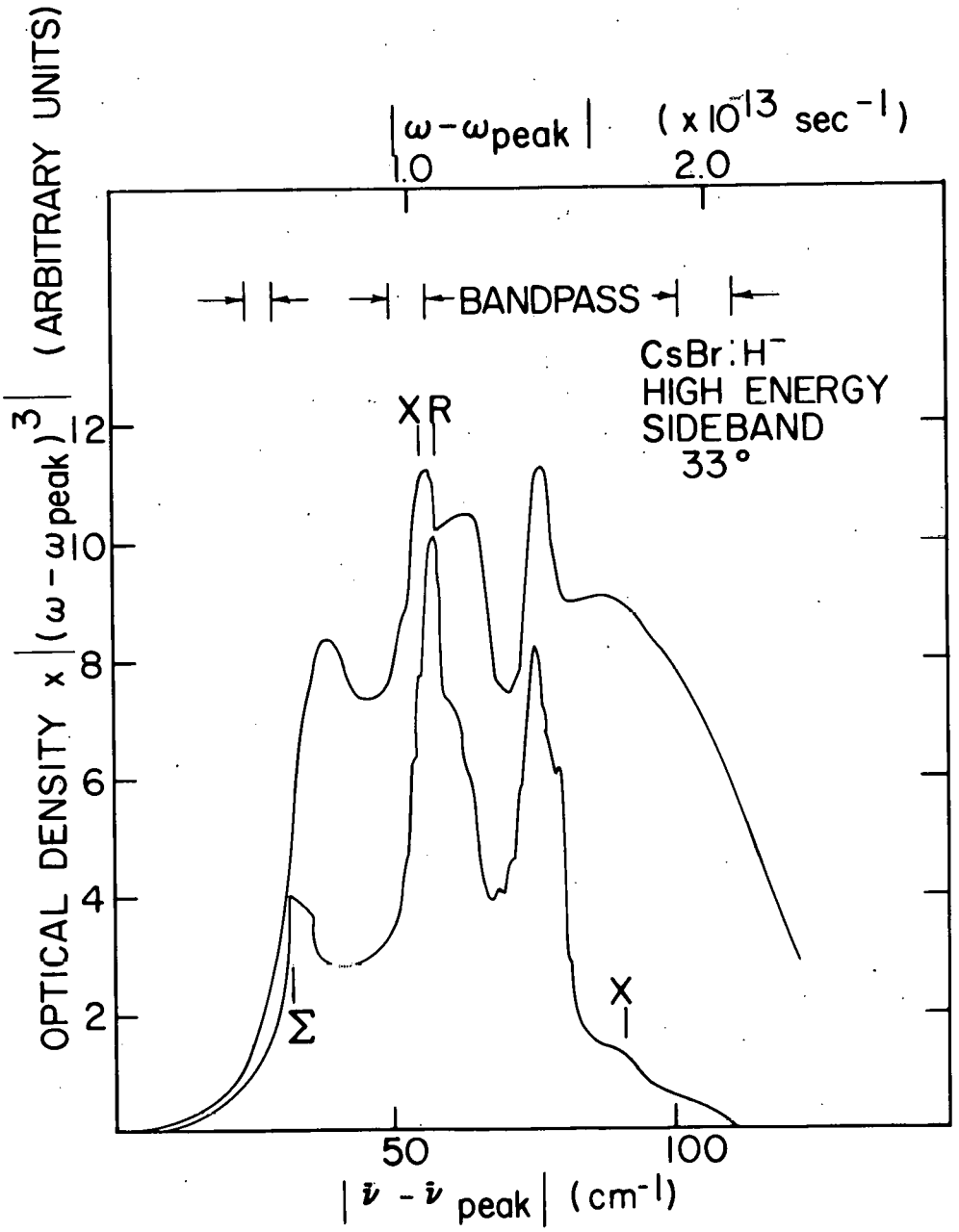

Figure 14. High energy sideband of the CsBr hydrogen U-center with an ω^3 weighting factor. The lower curve is Karo and Hardy's DD(-) one-phonon density of states

The CsI U-center has some features which are not as easily explained. Figures 15 and 16 show the local mode absorptions of CsI:H^- and CsI:D^-. The significant difference from the CsBr centers is the rapid increase of a high energy shoulder with temperature. This asymmetry appears to be characteristic of CsI. It appears in all samples measured and the relative magnitude is the same at all concentrations within the relatively small range used. It appears in CsI purchased at widely different times and will all monochromator-detector combinations. It does not change with repeated heating and cooling cycles or with annealing near the melting point and quenching. The only published data on CsI U-centers (10) are for higher temperatures but they also show the asymmetry.

The temperature dependences of measured properties are given in Figures 17 and 18. The choice of a significant half-width is not apparent. The asymmetry persists to very low temperatures. In addition, the measured curve is neither Lorentzian nor Gaussian on either side. For these reasons correction tables are not strictly applicable. An approximation of the half-width corrected for bandpass was obtained by fitting a symmetric band to each side. The vertical lines in Figure 17 indicate a reasonable range of corrected widths obtained this way. At higher temperatures the absorption becomes so wide no corrections are required. In these cases,

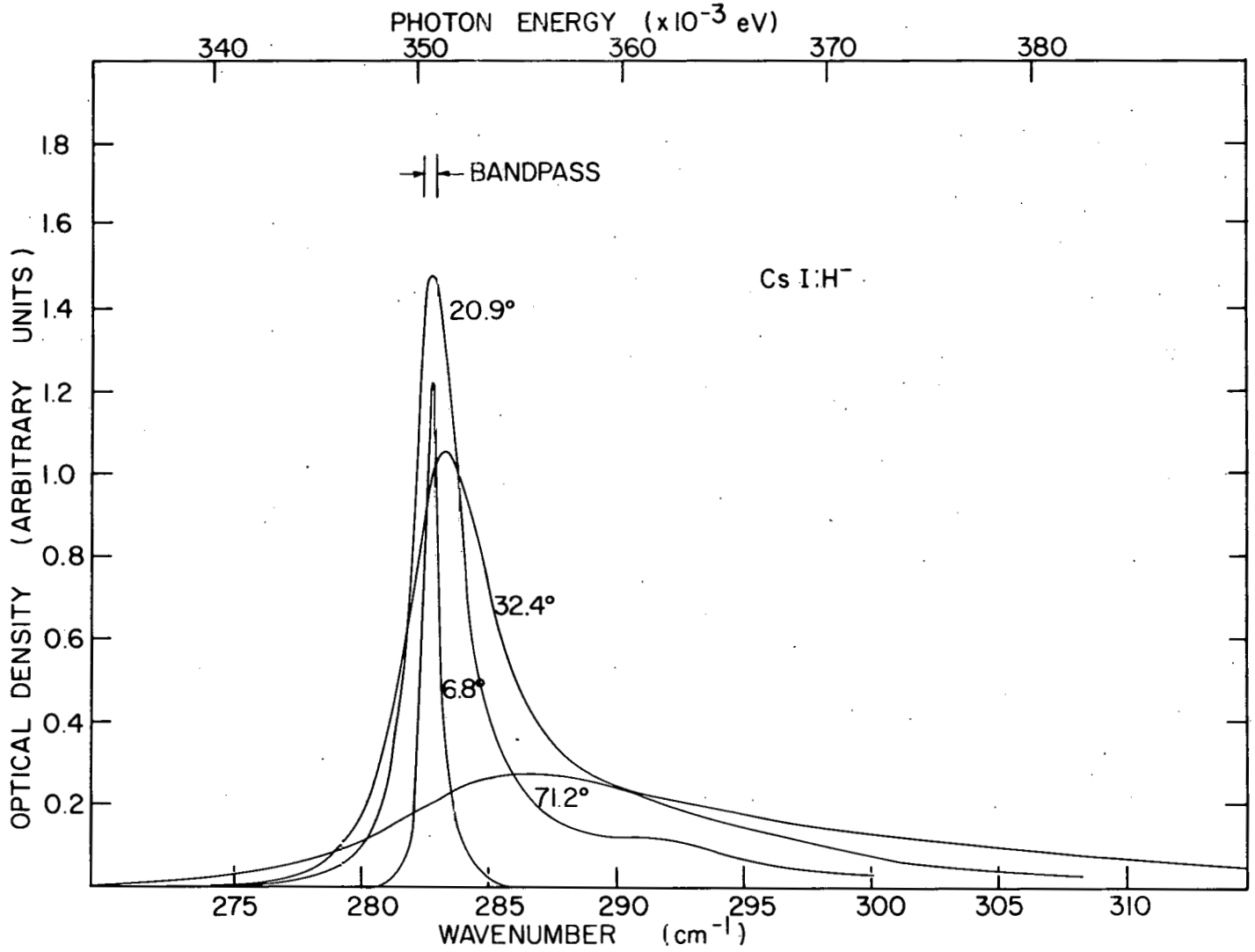

Figure 15. Examples of main peak absorptions due to CsI hydrogen U-centers

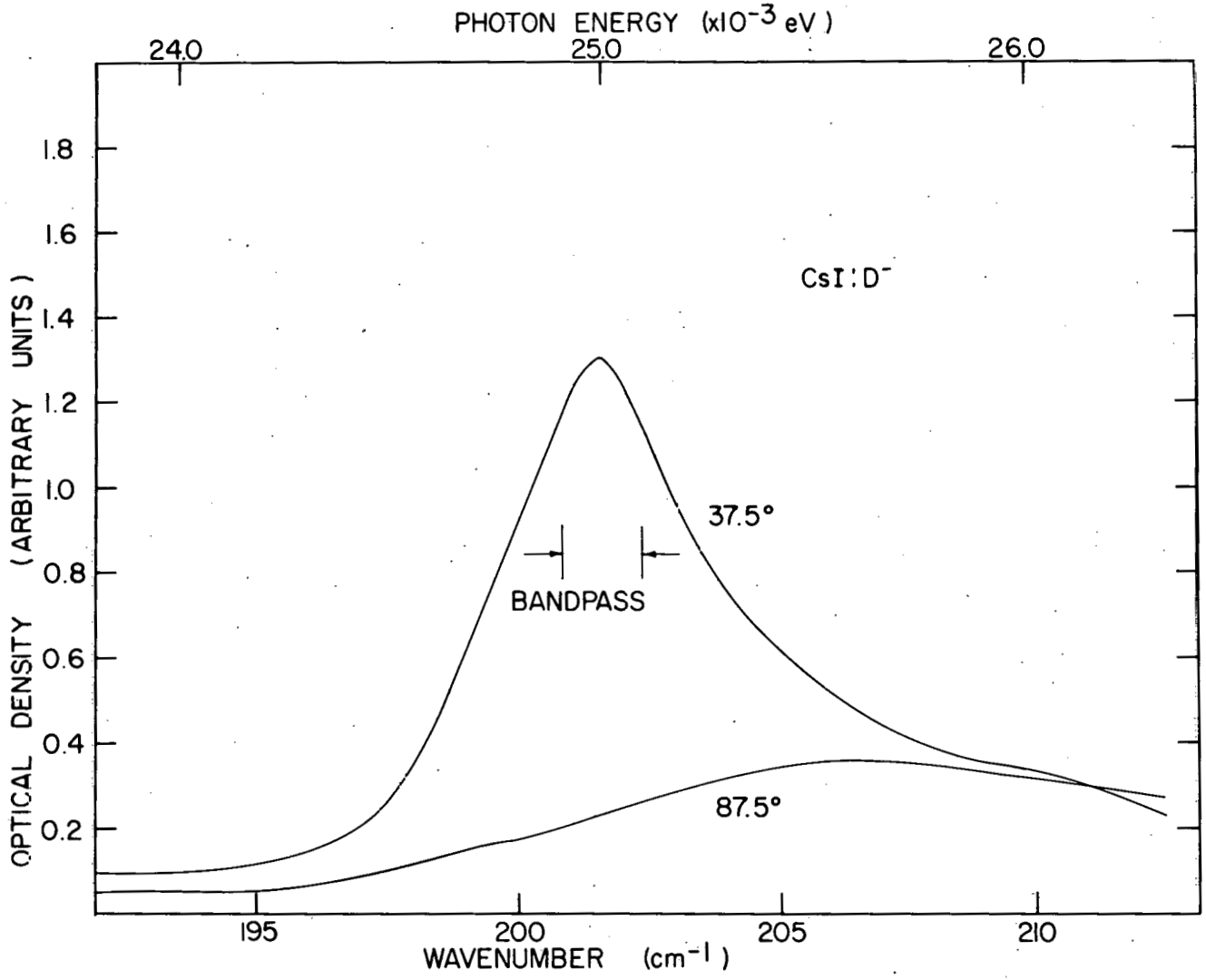

Figure 16. Examples of main peak absorptions due to CsI deuterium U-centers

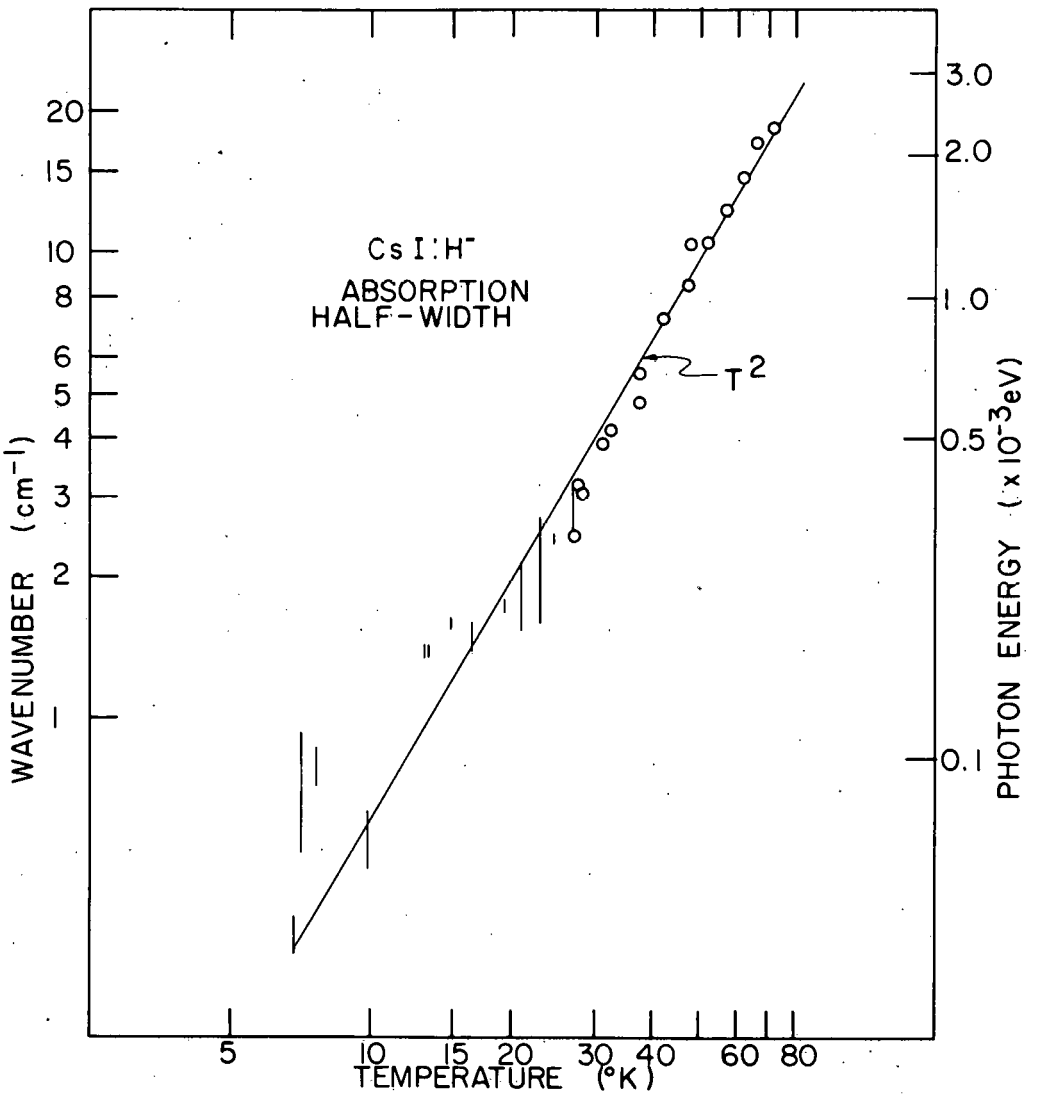

Figure 17. Log-log plot of CsI hydrogen U-center absorption half-width as a function of temperature. See text for bandpass corrections used.

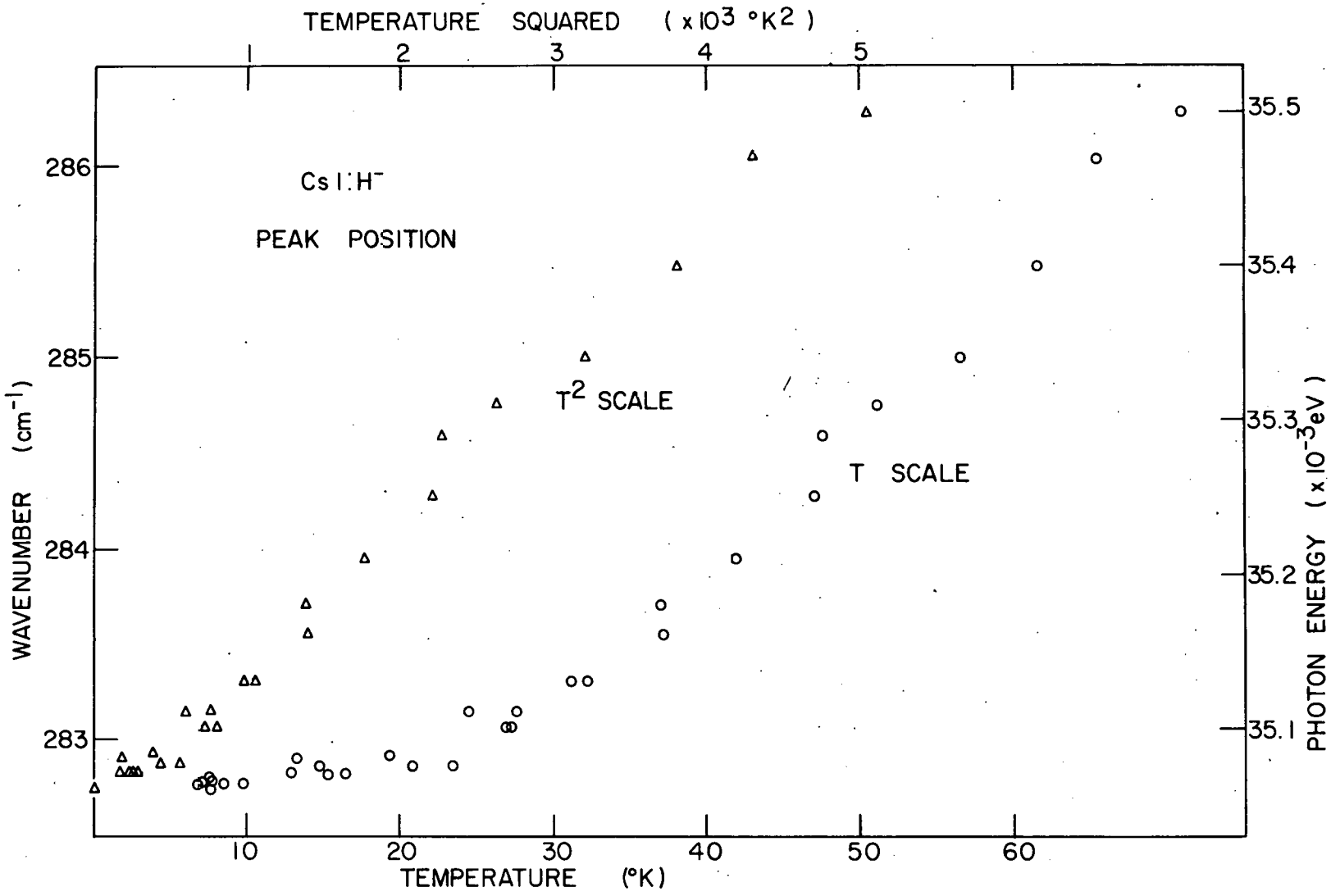

Figure 18. Shift of the CsI hydrogen U-center absorption maximum as a function of temperature and temperature squared

the overall width of the asymmetric band is plotted even though this may not be the physically significant width. The measured widths may be fit reasonably well by a T^2 temperature dependence. The width increases so rapidly that measurements were not made above 75^o.

The absorption of the D^- center was only measured at two temperatures. The degree of asymmetry appears to be the same as for the H^- center. In fact, the half-width of the absorption at 37^o is the same for the two isotopes to well within the uncertainty of the measurement. The significance of this is related to the validity of measuring the width of the entire curve.

A similar ambiguity arises in deciding how to represent the temperature dependence of the peak energy. The energies plotted in Figure 18 are those of the entire curve. Over most of the range the shift has a T^2 dependence and has a net shift more than five times that of CsBr. A low temperature limit to the local mode energy of CsI:D^- was not measured. The ratio of the peak energies at 37^o, however, gives an isotope shift of 1.41.

The high energy sideband is weak and is generally obscured by the high energy shoulder. The low energy sideband occurs in a region where sufficiently accurate measurements could not be made. The absorption on the high energy side of the local mode is given in Figure 19. Consistently measure-

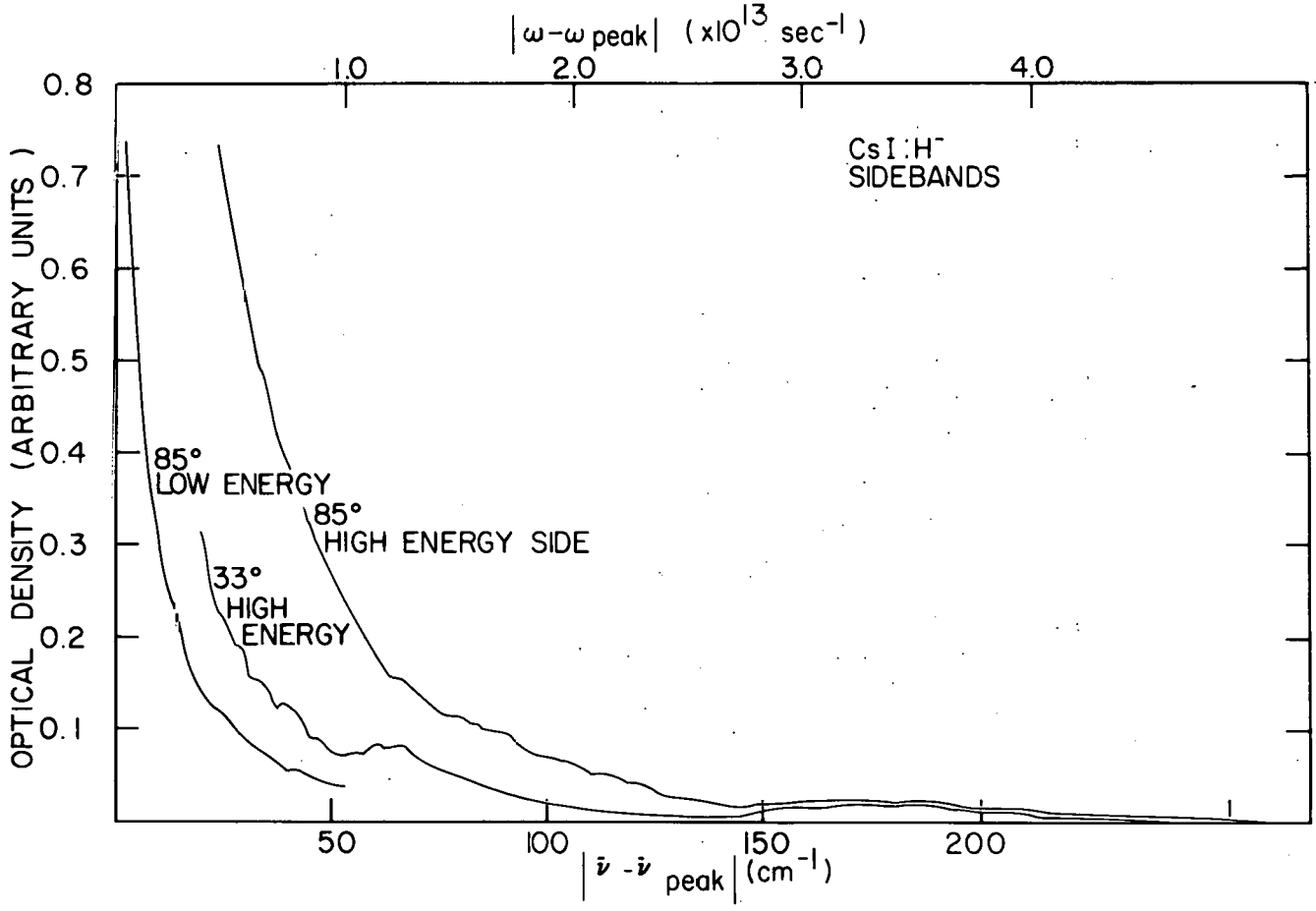

Figure 19. Sidebands of the CsI hydrogen U-center

able absorption occurs out to an energy three times that of the maximum lattice phonon energy. In Figure 20 the low temperature sideband is given with an $(\omega-\omega_H)^3$ weighting factor. It is meaningless to attach physical significance to this curve for two reasons. First, until the origin of the high energy asymmetry is known, the appropriate origin for this weighting factor is unknown. The measurement might represent a large series of sidebands. Secondly, determining the perturbed one phonon density of states for a given model requires knowledge of the symmetry of the defect mode. In spite of these unknowns, a Karo and Hardy DD(-) density of states is given in Figure 20. Some of the permitted modes are marked assuming cubic (Γ_{15}^-) symmetry of the defect.

An obvious first question is whether what was measured was in fact a U-center. Energies of U-centers may be plotted in many ways in attempts to derive a rule of thumb. One is to make an Ivey plot--that is to plot the log of the peak energy vs. the log of the lattice constant. U-centers in CsCl structure salts give a line with a different slope than those in NaCl lattices as might be expected, but the measured energies do fit a straight line. A variation is to plot log energy vs. log nearest-neighbor distance. This gives a set of parallel lines through the alkali groups and again CsI is at the predicted energy. A third variation is to plot negative ion atomic weight vs. energy of the local mode. This time a

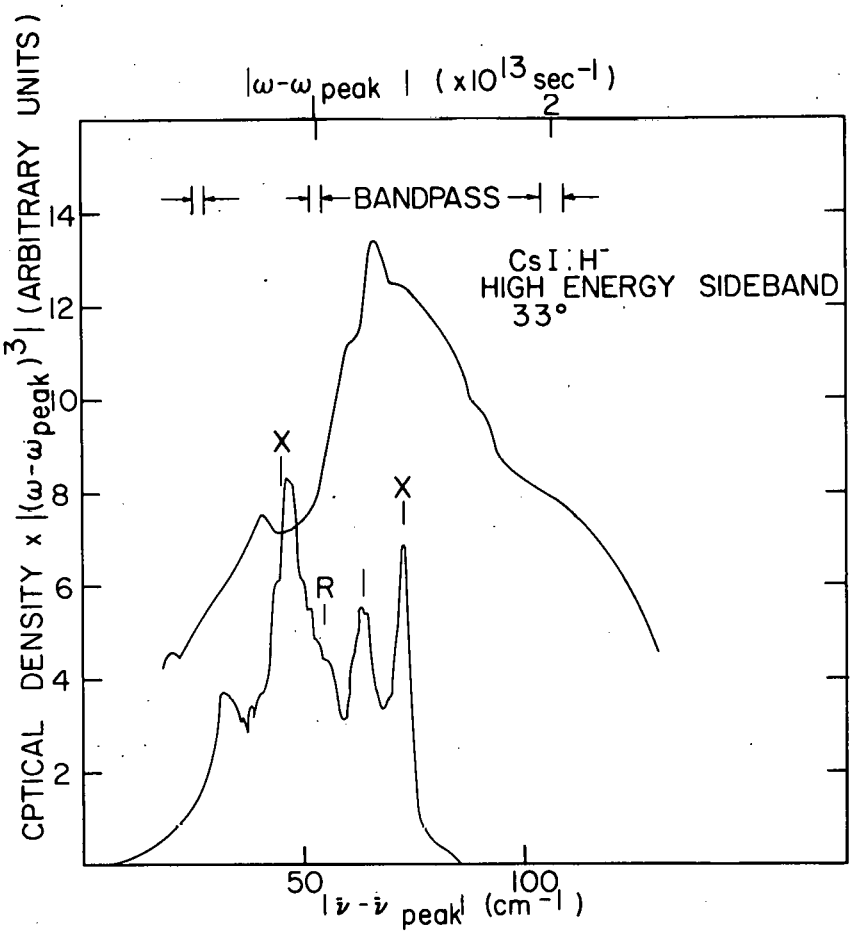

Figure 20. High energy sideband of the CsI hydrogen U-center with an ω^3 weighting factor. The lower curve is Karo and Hardy's DD(-) one-phonon density of states

set of parallel lines results which predict a slightly higher energy (about 4%) for CsI than is measured. The least that may be said is that the measured absorption energy is not unreasonable for a CsI U-center. This together with the other properties of the measured absorption would indicate that it is a U-center. All explanations of the asymmetry have at least one major flaw. These will be pointed out in the following discussions of possible explanations.

To establish terminology, consider Figure 21. An image of the low energy side has been subtracted from the high energy side. This resolves the measured absorption into a center symmetric portion and an extra high energy contribution. The energies involved are such that the splitting of the peaks of the two parts varies from 4 to 8 cm^{-1} with temperature. It is important to note the effect of this arbitrary subtraction. One could alternately subtract a symmetric curve which remained centered at the low temperature peak energy. In this case, the "extra" portion retains approximately the same shape but grows in strength at the expense of the symmetric part.

The first impulse is to attribute an unusually wide, distorted absorption to internal strains or impurities. There is only slight support for a model in which some of the H^- ions are on interstitial sites (U_1-centers). The room temperature ultra-violet absorption shows only the characteristic

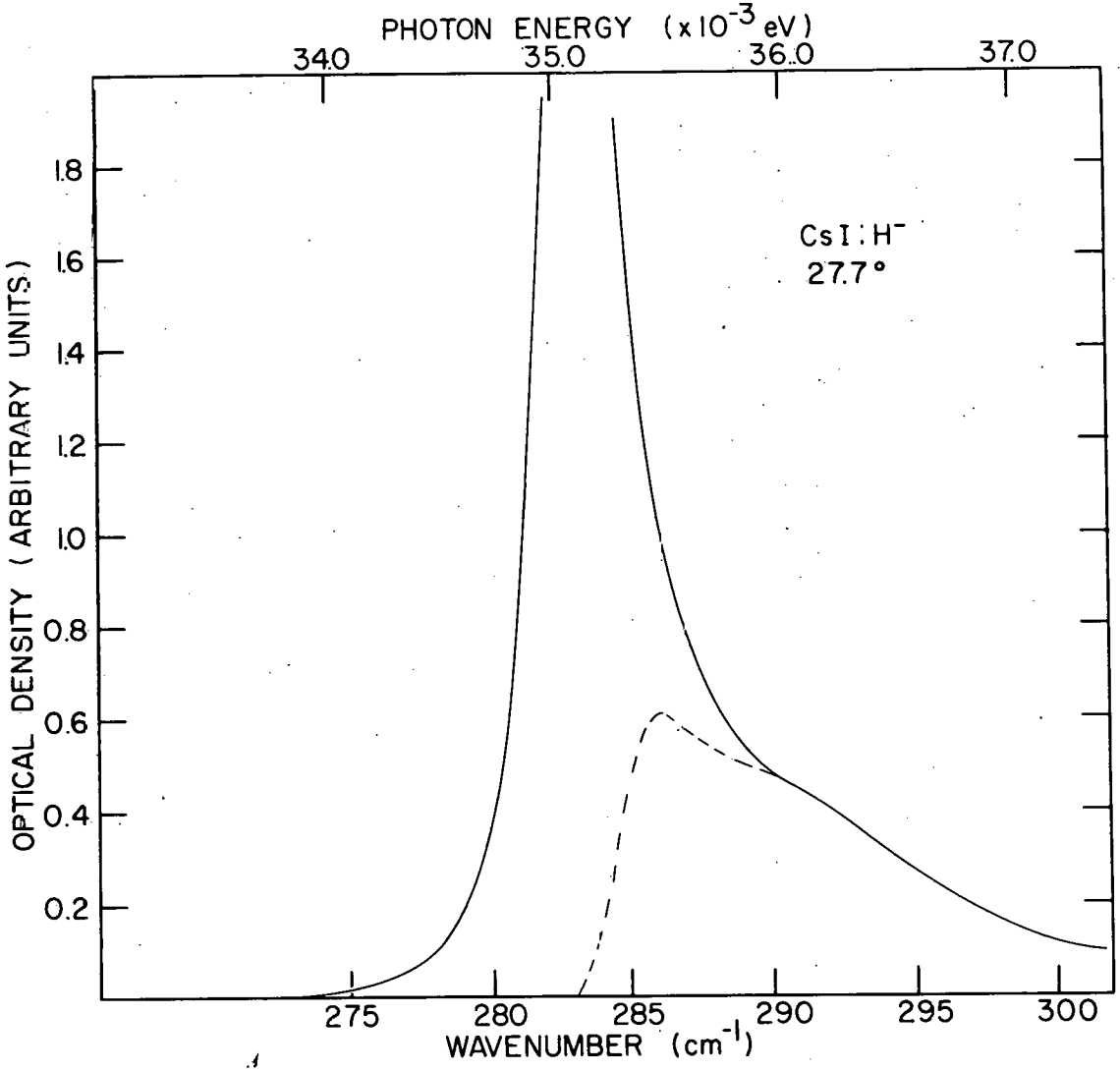

Figure 21. CsI hydrogen U-center absorption showing the asymmetric portion

U-band, not the lower energy U_1 absorption. Fritz (31) has studied the infrared properties of U_1-centers in KBr. He reports what appear to be three types of H^- interstitials with absorptions occurring between ω_H and $2\omega_H$. The interstitials are created by irradiating the sample in the U-band at a low temperature (80°). The interstitials anneal out at higher temperatures and all are gone by room temperature. CsI does show a weak absorption between $1.5\omega_H$ and $2\omega_H$. The asymmetry is so strong on the other hand, that at $50^\circ K$ half of the hydrogen would have to be interstitial. There is no evidence for a U_1-center concentration of this magnitude.

A symmetrical distribution of strains should cause broadening that persists to low temperatures. The measured absorption becomes very narrow at low temperature. In addition it is difficult to reconcile sample-to-sample uniformity with the effect of strains. Strains or impurities which remove the degeneracy might produce the asymmetry. One would expect, however, the structure to sharpen and ultimately split at low temperature. Attempts to produce splitting in CaF_2 structure U-centers have shown the necessary uniaxial strain is so great that this does not seem to be a reasonable mechanism (17). One further comment applies to many of the mechanisms proposed. A normal U-center is at a site of O_h symmetry. Symmetry considerations then forbid second harmonic absorption. If the site of the H^- is reduced to, say, tetrag-

onal symmetry, a second harmonic is possible (17). No trace of a second harmonic is seen in CsI. If it were present at all it would have to be several orders of magnitude smaller than the fundamental.

The temperature dependence of the asymmetry suggests another model. Unfortunately temperature dependence is the only thing in its favor. The anharmonic potential may produce difference sidebands (Equation 2-12c). Because of the requirement of a thermally excited lattice phonon in the process, the strength would go to zero at T = 0. Difference phonon absorption has been seen in pure NaCl structure materials (32). In that work the phonons involved were transverse optic and transverse acoustic. In Karo and Hardy's DD(-) model, the optical and acoustic branches are each triply degenerate at R with a splitting of about 5 cm^{-1}. However, the branches are of opposite parity (5); second sidebands should be weaker than single sidebands which are already weak, and the difference sidebands ought to occur on both sides of the local mode.

Since the local mode oscillator is in an anharmonic potential, the energy levels are not evenly spaced. Transitions from a thermally excited n = 1 level to a n = 2 level would have slightly different energy than the fundamental absorption. The asymmetry is seen at such a low temperature relative to the local mode energy (equivalent temperature 408^{o}) that only a negligible portion of the centers could be

thermally excited.

A final possibility is that as the crystal warms, the lattice expands and it becomes energetically favorable for the H^- ion to move off-center. The result may be discussed in terms of ferroelectrics. Relative displacements of ionic sublattices produce a dipole moment even in the absence of an electric field. Equivalently, the displacement could be considered to give rise to a very low frequency transverse-optic mode. The mode is at low frequency since the local electric field tends to increase the amplitude of the deformation, lowering the frequency.

The absorption asymmetry might be caused by coupling of the local mode to this low frequency mode. The frequencies involved are reasonable. Klein's (12) theory for sidebands predicts that if the coupling is due to the anharmonic force the sidebands will grow in strength at the expense of the local mode peak. If the coupling is through the second-order dipole moment, the net absorption will increase. The total absorption of the CsI U-center is essentially constant.

There are several problems with this explanation. Usually a defect is frozen into an off-center site at low temperature and as the lattice warms, thermal motion restores full cubic symmetry. Those ferroelectrics that contain hydrogen (potassium dihydrogen phosphate group) show a strong isotope effect. The Curie temperature and saturation polari-

zation both show a factor of nearly two dependence. Finally, if the shoulder is a form of sideband, why is there no equivalent absorption on the low energy side?

At this time, therefore, it must be said that the details of the CsI U-center absorption lack an explanation. There are several possible courses of future work. It would be interesting to see if splitting could be produced with pressure. It would also be interesting to look at U-centers produced with an intermediate step other than additive coloration. The apparent lack of an isotope effect indicates that it might be worthwhile to pursue a detailed study of the properties of pure CsI as a function of temperature and pressure.

SUMMARY

The temperature dependence of the U-center absorption in CsBr and CsI was measured. The small mass of the hydride ion relative to the normal ionic masses in the lattice produced a local mode with a frequency more than four times that of the maximum frequency lattice phonon. Substituting deuterium decreased the local mode frequency by the square root of two. In addition to the local mode absorption, coupling between the local mode and those lattice phonons permitted by symmetry produced sidebands which were the absorption of the local mode with absorption or emission of lattice phonon.

The half-width of the CsBr local mode absorption increased with a T^2 temperature dependence. At high temperatures the width was due to modulation broadening produced by the fourth order anharmonic potential term. The mass dependent coefficient of the potential caused the hydride half-width to be twice that of the deuteride center. At low temperatures the modulation broadening went to zero and the residual half-width was determined by decomposition into lattice modes. In this limit, the deuteride width was larger. This was a result of the relative strength of the two potential terms involved (fifth order for H^- and fourth order for D^-) and the fact that the one-phonon density of states of CsBr is larger at the average phonon frequency of the lattice modes involved in the deuterium local mode

decomposition. The peak of the local mode absorption shifted to higher energy with a linear temperature dependence. Substituting deuterium for hydrogen increased the shift by 1.48. The physical origin of the shift was not established although at high temperatures there was apparently a contribution due to thermal expansion. The high energy sideband (produced by a local mode plus a lattice phonon) was plotted with a weighting factor of the lattice phonon frequency cubed. The result was in good agreement with the one-phonon density of states calculated by Karo and Hardy using their DD(-) model.

The main peak absorption of the CsI U-centers had a high energy shoulder which increased rapidly in strength with increasing temperature. No satisfactory explanation of this feature was found. As a result, it was impossible to give a detailed explanation of the temperature dependence of the half-width or shift of peak energy.

BIBLIOGRAPHY

1. J. H. Schulman and W. D. Compton, Color centers in solids (The Macmillan Company, New York, 1962, p. 163.
2. G. Schaefer, J. Phys. Chem. Solids 12, 233 (1960).
3. R. Loudon, Proc. Phys. Soc. 84, 379 (1964).
4. G. F. Koster, in Solid state physics 5, edited by F. Seitz and D. Turnbull (Academic Press Inc., New York, 1957), p. 174.
5. J. L. Warren, Rev. Mod. Phys. 40, 38 (1968).
6. A. M. Karo and J. R. Hardy, J. Chem. Phys. 48, 3173 (1968).
7. E. R. Cowley and A. Okazaki, Proc. Roy. Soc. A300, 45 (1967).
8. J. V. Bauer, M. S. thesis, Iowa State University, 1966 (unpublished).
9. S. S. Mitra and Y. Brada, Phys. Rev. 145, 626 (1966).
10. H. Dotsch and S. S. Mitra, Phys. Rev. 178, 1492 (1969).
11. Localized excitations in solids, edited by R. F. Wallis (Plenum Press, New York, 1968).
12. M. V. Klein, In Physics of color centers, edited by W. Beall Fowler (Academic Press, New York, 1968), p. 429.
13. E. Hanamura and T. Inui, J. Phys. Soc. Japan 18, 690 (1963).
14. R. Kubo, J. Phys. Soc. Japan 12, 570 (1957).
15. P. Vergnat, J. Claudel, A. Hadni, P. Strimer, and F. Vermillard, J. de Phys. 30, 723 (1969).
16. R. P. Lowndes, Phys. Rev. B 1, 2754 (1970).
17. R. J. Elliott, W. Hayes, G. D. Jones, H. F. MacDonald, and C. T. Sennett, Proc. Roy. Soc. A289, 1 (1965).
18. T. Timusk and M. V. Klein, Phys. Rev. 141, 664 (1966).

19. T. Gethins, T. Timusk, and E. J. Woll, Phys. Rev. 157, 744 (1967).

20. M. Lax and E. Burstein, Phys. Rev. 97, 39 (1955).

21. H. Bilz, B. Fritz, and D. Strauch, J. Phys. (Paris) Suppl. 27, C2-3 (1966).

22. R. Wehner, Phys. Stat. Sol. 15, 725 (1966).

23. C. Z. van Doorn, Rev. Sci. Instr. 32, 755 (1961).

24. L. A. Lott, Ph.D. thesis, Iowa State University, 1965 (unpublished).

25. H. M. Randall, D. M. Dennison, H. Ginsburg, and L. R. Weber, Phys. Rev. 52, 160 (1937).

26. D. A. Ramsay, J. Am. Chem. Soc. 74, 72 (1954).

27. I. M. Mills, J. R. Scherer, B. Crawford, Jr., and M. Youngquist, J. Opt. Soc. Am. 45, 785 (1955).

28. A. R. Downie, M. C. Magoon, T. Purcell, and B. Crawford, Jr., J. Opt. Soc. Am. 43, 941 (1953).

29. M. A. Ivanov, M. A. Krivoglaz, D. N. Mirlin, and I. I. Reshina, Soviet Phys.-Solid State 8, 150 (1966).

30. P. A. Jansson, J. Opt. Soc. Am. 60, 184 (1970).

31. B. Fritz, J. Phys. Chem. Solids 23, 375 (1962).

32. R. Stolen and K. Dransfeld, Phys. Rev. 139, A 1295 (1965).

33. G. W. Stroke, Handbuch der Physik 29, 528 (1967).

34. P. H. van Cittert, Z. Physik 65, 547 (1930).

35. B. D. Saksena, D. R. Pahwa, M. M. Pradham, and K. Lai, Infrared Phys. 9, 11 (1969).

36. P. C. von Planta, J. Opt. Soc. Am. 47, 629 (1957).

37. F. Kneubuhl, Appl. Opt. 8, 505 (1969).

APPENDIX

The bulk of serious writing on resolution and slit functions has been concerned with the use of a spectograph to record atomic emission spectra on film (Stroke (33) and references therein). This instrument is also fundamental to understanding a spectrometer operated in an energy limited mode. A spectrometer is energy limited when the detector sensitivity requires the slits to be opened to pass a wider range of wavelengths than the minimum defined by the physical characteristics of the monochromator.

A plane diffraction grating used in a Littrow mount has almost equal angles of incidence and diffraction. Assuming incoherent, monochromatic light, the grating may be considered to be a properly oriented mirror. Given the angle of incidence θ and the ruled width W the grating presents an aperture A where

$$A = W\cos\theta. \qquad \text{(A-1)}$$

A rectangular slip which is long with respect to its width A produces a diffraction pattern with an intensity distribution (Figure 22)

$$I(x) = \left(\frac{\sin x}{x}\right)^2. \qquad \text{(A-2)}$$

Where x represents π times a width in units of $\lambda f/A$. The first minima in the exit plane occur at $\pm\lambda f/A$ where f is the focal length of the system. The half-width of the principal maximum is $0.86\ \lambda f/A$. Neglecting the finite height of the grating, this

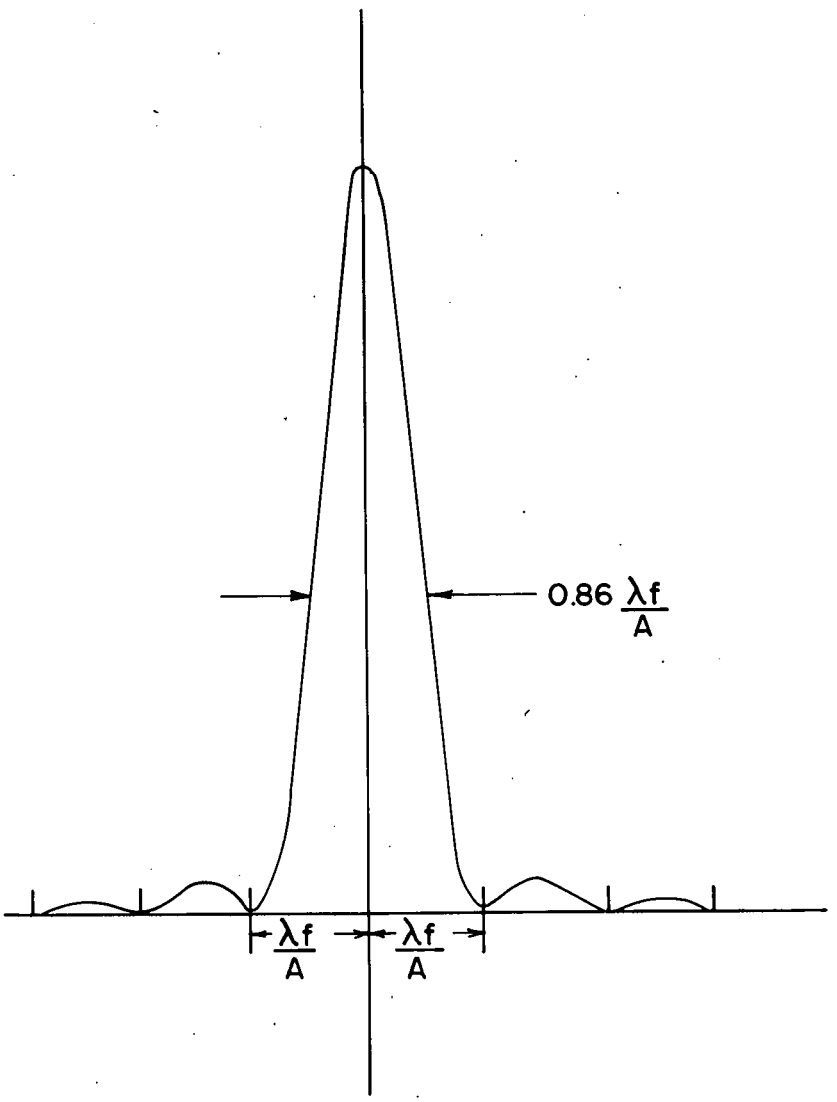

Figure 22. Diffraction pattern of an infinitely narrow slit

would be the image on the film if the grating were illuminated uniformly by an arbitrarily narrow entrance slit. As an example, if A = 5 cm, f = 27 cm, and $\lambda = 30\mu$, then $\lambda f/A$ = .16 mm.

Consider next the role of the entrance slit. It too will produce a diffraction pattern of width approximately $\lambda f/s$. If s, the slit width, is very small the resulting pattern will be much wider than the aperture A. The pattern in the exit plane will have minimum width but the intensity will be low. If the slit is opened until $\lambda f/s \approx A$ (s = .16 mm in our example), the portion of the central maximum containing most of the energy will fill the grating. The image in the exit plane, however, will now be influenced by the finite slit. Rigorously, it will be the convolution of the grating aperture diffraction pattern with the distribution of intensity across the slit. This has been calculated by van Cittert (34) and is shown in Figure 23 taken from Stroke (33).

The characteristics of the grating determine the separation of two adjacent wavelengths. The basic grating equation may be written as

$$n\lambda = d(\sin\theta_{ent.} + \sin\theta_{exit}) \qquad (A-3)$$

where n is the order and d is the line spacing. With a Littrow mount, while the angles are essentially equal, the quantity of interest is the effect of a small change in θ_{exit} while keeping the entrance slit and grating fixed.

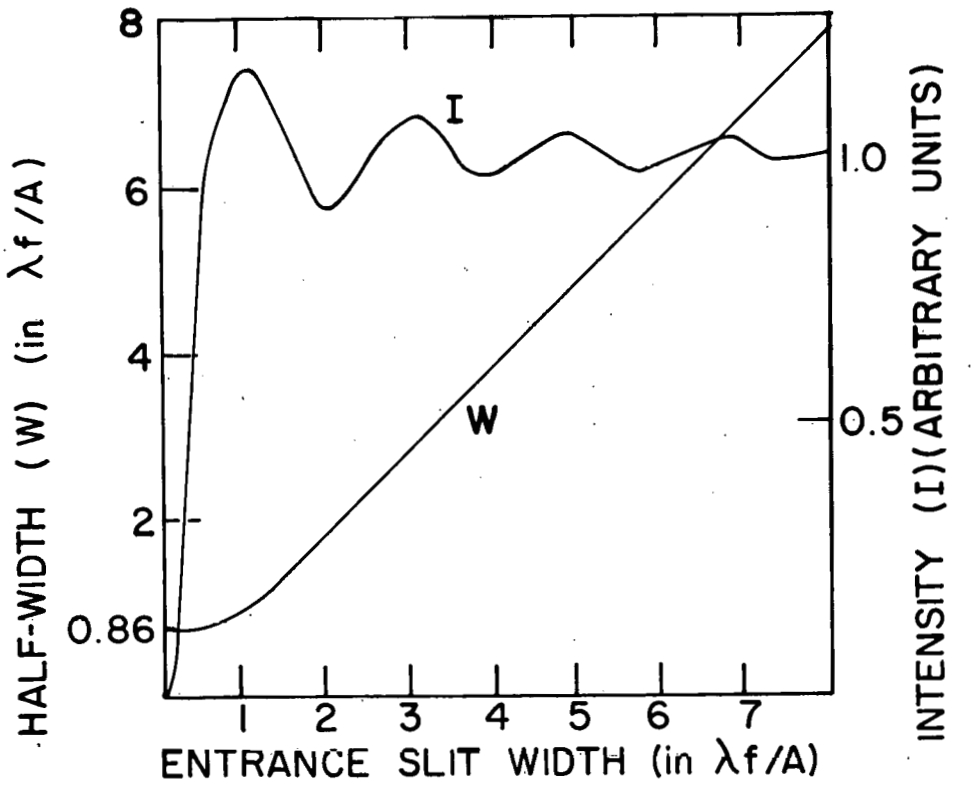

Figure 23. Image intensity and half-width in the exit plane as a function of entrance slit width assuming incoherent radiation

$$n\Delta\lambda = d(\cos\theta_{exit})\ \Delta\theta_{exit} \qquad \text{(A-4)}$$

The Rayleigh criterion for the resolution of two adjacent lines is that the diffraction maximum of one fall on the first minimum of the other. If the slits are very narrow the pattern in the exit plane will be a pure single slit diffraction pattern. To be resolved, therefore, the two maxima must be separated by $\lambda f/A$. Resolving power is defined as

$$R_g = \left|\frac{\lambda}{\Delta\lambda}\right| = \left|\frac{\tilde{\nu}}{\Delta\tilde{\nu}}\right| \qquad \text{(A-5)}$$

where $\tilde{\nu}$ is a wave number or reciprocal wavelength. From the grating equation, the angular dispersion (δ) is

$$\delta = \frac{d\ \theta_{exit}}{d\ \lambda} = \frac{n}{d\ \cos\theta}\ . \qquad \text{(A-6)}$$

The label on θ has been dropped since $\theta_{entrance} = \theta_{exit}$. From the Rayleigh criterion

$$\frac{\lambda f}{A} = \Delta x = f\Delta\theta. \qquad \text{(A-7)}$$

Then

$$\frac{\lambda}{A} = \Delta\theta = \frac{d\ \theta}{d\ \lambda}\ \Delta\lambda = \frac{2\ \tan\theta}{\lambda}\ \Delta\lambda. \qquad \text{(A-8)}$$

Therefore

$$R_g = \left|\frac{2\ W\ \sin\theta}{\lambda}\right|. \qquad \text{(A-9)}$$

To put this in a more common form, substitute

$$W = ND \qquad \text{and} \qquad 2\sin\theta = n\lambda/d.$$

Then $$R_g = nN \qquad \text{or} \qquad \Delta\tilde{\nu} = \tilde{\nu}/nN. \qquad \text{(A-10)}$$

Consider the effect of the spectograph being operated energy limited with a continuous source. The single slit diffraction pattern would have to be convolved with the slit function to obtain the pattern in the exit plane for a single wavelength. This pattern would give the parameter, containing information about the slit width, to be used in the Rayleigh criterion.

The next step is to apply this to a spectrometer being operated with equal entrance and exit slits whose width may be many times the diffraction width. For the single slit spectograph, the slit function was a rectangle with width equal to the slit width. With two slits the slit function is the convolution of two rectangles. If the two slits are equal, this will produce the well-known triangular slit function. The dispersive element determines the width of this triangle.

For a grating

$$R = \left|\lambda/\Delta\lambda\right| = \frac{2d\ \sin\theta/n}{\frac{2d\ \cos\theta}{n}\ \Delta\theta} \qquad \text{(A-11)}$$

where $\Delta\theta = s/2f$.

The triangle will have a width at half maximum

$$\Delta\bar{\nu} = \bar{\nu}\ \frac{s\ \cos\theta}{2f\ \sin\theta} \qquad \text{(A-12)}$$

The treatment of a prism spectrometer is only slightly more complicated. Assume that equal slits are used and the

prism is used at minimum deviation. Standard optics texts derive the resolving power of a prism as

$$R_p = \left| \bar{\nu} / \Delta\bar{\nu} \right| = b \cdot \frac{dn}{d\lambda} \quad \text{or} \quad \Delta\bar{\nu} = \bar{\nu} / b \cdot \frac{dn}{d\lambda} \qquad \text{(A-13)}$$

where b is the base length of the prism. In a Littrow mount the beam traverses the prism twice, effectively increasing the base to 2b.

The slit function is again a triangle with a width determined by the dispersive properties of the prism. A derivation has recently been published by Saksena (35). The result is straightforward and is given by the first term of the Williams relation (35).

$$\Delta\bar{\nu} = \frac{\bar{\nu}^2 (1 - n^2 \sin^2 \frac{1}{2}a)^{\frac{1}{2}}}{8 \sin \frac{a}{2} \left(\frac{dn}{d\lambda}\right)} \frac{2s}{f} \qquad \text{(A-14)}$$

where n is the index of refraction and a is the prism angle. This is the width of the triangle at half maximum.

The bandpass function is the convolution of the diffraction pattern of the grating or prism aperture and a triangular slit function of width determined above. Thus the bandpass function will appear to be single slit diffraction pattern for small slits, proceed through a Gaussian-like form and become a slightly smoothed triangle for large slit widths. This is also the experimental finding of von Planta (36).

The resolution of the spectrometer may be calculated

using the result of the convolution and the Rayleigh criterion. By introducing a function of the slit width it can be written as

$$\Delta\tilde{\nu} = \Delta\tilde{\nu}_{\text{slit function}} + F(s)\Delta\tilde{\nu}_{\text{prism}}. \qquad \text{(A-15)}$$

F(s) is a number less than one which may be calculated. Some authors let F(s) equal one (e.g. Kneubuhl (37) for gratings). Williams gives general limits for F(s). Saksena performed the calculation for specific conditions and gives values for a wide range of slit widths.

For conditions existing in this work, F(s) is approximately 0.8. The bandpass function is basically triangular as the slits were generally three times the diffraction width.

ACKNOWLEDGEMENT

The author would like to thank past and present members of Crystal Physics Group 8, especially D. A. Robinson, A. D. Brothers and J. V. Bauer, for their suggestions and assistance during this work.